Energy, Mines and Resources Canada | Énergie, Mines et Ressources Canada

CANMET

Canada Centre for Mineral and Energy Technology | Centre canadien de la technologie des minéraux et de l'énergie

TOUGHNESS OF WELD METALS FOR FABRICATION OF COLD MARINE STRUCTURES AND VESSELS. Part 1: SHIELDED METAL ARC WELDING

J.E.M.BRAID and J.A.GIANETTO
WELDING SECTION

APRIL 1988

THIS WORK WAS SUPPORTED BY THE FEDERAL PANEL ON ENERGY R & D (PERD)

72 pp

METALS TECHNOLOGY LABORATORIES
REPORT: MTL 88-21(TR)

88-04997/

METALS TEHCNOLOGY LABORATORIES
REPORT: MTL 88-21(TR)

TOUGHNESS OF WELD METALS FOR FABRICATION OF COLD MARINE STRUCTURES AND VESSELS. PART 1: SHIELDED METALARC WELDING

by

J.E.M. BRAID and J.A. GIANETTO

ABSTRACT

A series of 20 butt welds in 20 mm thick steel plate was made using commercially available shielded metal-arc welding (SMAW) electrodes selected from major manufacturers in Europe, the United States and Canada of CSA E48016, E48018 and E55018 type C-Mn and C-Mn-Ni compositions. The welds were evaluated, in terms of microstructure and toughness, for their suitability in fabricating structures with -20°C to -50°C design temperatures and to identify areas where improvements can be made in consumable design. Few of the C-Mn electrodes evaluated met a 0.08 mm crack tip opening displacement (CTOD) requirement for -30°C design temperatures while approximately half met this requirement at -10°C. The addition of nickel, up to 3.5%, improves toughness and four of the E55018-C1 and C2 electrodes tested met the requirements at -30°C.

Low temperature fracture occurred by cleavage initiation at large, >1 μm diam., inclusions primarily located in grain boundary ferrite of as- deposited weld metal. Improvements in toughness were associated with high proportions of acicular ferrite microstructures and low numbers of large inclusions. Improvements in toughness should be possible with further optimization of electrode coatings to eliminate large inclusions and increase proportions of acicular ferrite through Ti, B and Ni additions and providing optimal nucleation sites.

LABORATOIRES DE LA TECHNOLOGIE DES MÉTAUX
RAPPORT MTL 88-21(TR)

TÉNACITÉ DES MÉTAUX DE SOUDURE DESTINÉS À LA FABRICATION DES STRUCTURES MARITIMES ET NAVIRES POUR RÉGIONS FROIDES. PARTIE 1: SOUDAGE À L'ARC MÉTALLIQUE AVEC ÉLECTRODE ENROBÉE

par

J.E.M. BRAID et J.A. GIANETTO

RÉSUMÉ

On a effectué une série de 20 soudages bout à bout, sur une tôle d'acier de 20 mm d'épaisseur, en employant des électrodes disponibles dans le commerce, pour soudage à l'arc métallique avec électrode enrobée; les électrodes sélectionnées provenaient de chez les principaux fabricants d'Europe, des États-Unis et du Canada, et leur composition était des types C-Mn et C-Mn-Ni, en conformité avec les normes ACNOR E48016, E48018 et E55018. On a évalué les soudures du point de vue de leur microstructure et de leur ténacité, et aussi des possibilités de les employer pour fabriquer des structures en présence de températures théoriques de -20°C à -50°C; on cherche aussi à identifier dans quels secteurs on peut apporter des améliorations aux modèles d'électrode fusible (consommable). Un petit nombre seulement des électrodes C-Mn évaluées ont satisfait à la norme de déplacement de l'ouverture de la pointe des fissures (CTOD), soit 0,08 mm. A une température théorique de -30°C, environ la moitié de ces électrodes ont satisfait à cette norme à -10°C. En ajoutant du nickel, jusqu'à une concentration de 3,5%, on a amélioré la ténacité; quatre des électrodes E55018-C1 et C2 testées ont satisfait à ces normes à -30°C.

A basse température, des criques de clivage sont apparues à l'emplacement d'inclusions importantes, de diamètre > 1 µm, principalement situées dans la ferrite de la périphérie des grains. On a associé les améliorations de la ténacité à l'existence de proportions élevées de microstructures de ferrite aciculaire et d'un petit nombre de grandes inclusions. Il doit être possible d'améliorer la ténacité en optimisant encore l'enrobage des électrodes, de façon à éliminer les grosses inclusions et à augmenter les proportions de ferrite aciculaire en ajoutant les éléments Ti, B et Ni, et en favorisant des sites optimaux de germination.

INTRODUCTION

Building offshore structures and ships for Canada's East Coast and Arctic regions will provide many new challenges. High strength, low alloy steels, of the C-Mn microalloy variety, are being developed with superior fracture toughness properties for use in Arctic climates. These steels, of yield strengths 350-500 MPa, will be suitable for both oil and gas production facilities and ships with ice breaking capability.

The welding technology currently available was developed for use in fabricating North Sea structures where the minimum design temperature is -10°C. However, minimum temperatures of -20°C and drifting ice, including icebergs, are design considerations for the Hibernia field. In the Arctic, minimum temperatures of -50°C and pack ice make the design of Beaufort Sea structures significantly different from those for the East Coast or North Sea. These low temperatures are also significant for icebreaking ships and supply vessels which must operate year round in these environments. The use of currently available welding consumables for offshore and Arctic structures and ships may be limited. Thus, welding consumables require evaluation to:

a) establish their suitability in fabricating structures with -20°C to -50°C design temperatures and
b) identify areas where improvements can be made in consumable design.

Several welding processes are used in fabricating offshore structures. Seventy-five per cent of tubular type structures are fabricated using the shielded-metal-arc welding (SMAW) process primarily for the all-position capability of this process as well as maintaining low hydrogen levels in the deposits. Submerged-arc welding (SAW) is used for seam welding of main can sections as well as deck sections while some of the out of position welds are completed using the Flux-Cored Arc Welding (FCAW) process (deck modules, etc.) Welding of Arctic structures and ships makes increased use of the SAW process since large panels are normally pre-fabricated in the flat position. However, for final assembly, manual and semi-automatic processes such as SMAW and FCAW are needed for their out-of-position capability. Owing to their current wide use in the industry, consumables for three processes (SMAW, FCAW and SAW) have been evaluated in terms of fracture toughness in the as-welded condition.

Twenty SMAW electrodes, 16 FCAW wires and 12 SAW wire/flux combinations were obtained from consumable manufacturers in Canada, the United States, Europe and Japan. The evaluation of the 16 FCAW wires was contracted to AMCA International and has recently been reported(1). Part 1 of this report deals with the evaluation of the SMAW electrodes while Part 2 will report on the evaluation of the 12 SAW consumables.

EXPERIMENTAL

MATERIAL AND CONSUMABLE SELECTION

A microalloyed C-Mn-Ni-V-Nb, 20 mm thick, steel conforming to CSA G40.21-350WT specification was chosen as the base material for all experimental welds. The chemical composition is listed in Table 1.

Commercially available shielded-metal-arc welding (SMAW) electrodes selected from major manufacturers in Europe, the United States and Canada, consisted of CSA E48016, E48018 and E55018 (AWS specifications E7016, E7018, and E8018) C-Mn and C-Mn-Ni compositions. Table 2 contains a list of the electrodes with their nominal compositions and corresponding weld identification.

WELDING PROCEDURE

In shielded-metal-arc welding good fracture toughness properties are most difficult to achieve while welding out-of-position. However, most of the critical joints in tubular structures, by their very nature, must be welded out-of-position, including vertical and overhead. Thus, any evaluation of welding consumables based on toughness should address this problem and also consider the following:

a) Joint preparation - groove angles, lands and root openings should represent a realistic joint with respect to welding induced strains, weld metal dilution, etc.
b) Heat Input - should realistically represent current production practice
c) Position - should represent the most demanding condition with respect to both welder ability and the effect on heat input and bead shape

d) Restraint - to minimize strain aging damage and represent restraint levels in practical joints

e) Preheat and Interpass Temperatures - as required to prevent cracking but should be the same for all the welds

f) Backgouging - normally done to remove strain age damaged root region material to improve overall joint toughness

g) Pass Sequence and Electrode Size - the size of electrode used, amount of weaving and pass sequence will (along with voltage, current and heat input) determine the size of the weld beads and hence the amounts of as-deposited and reheated microstructures. As-deposited microstructures for C-Mn structural steel weldments will generally have lower toughness relative to reheated microstructures (2-7). The type of microstructure and the number and size distribution of non-metallic inclusions is controlled primarily by the electrode coating formulation. Thus by testing welds with enough as-deposited microstructure the results will be more representative of an individual electrode.

After consideration of the above points and several trials welds the following welding procedure was developed.

Position:	Vertical-up (3G)
Plate Size:	600 mm x 1200 mm x 20 mm thick
Joint Preparation:	Single V-45° included angle
	2 mm land
	3.2 mm root opening
Electrode Size:	3.2 mm - all passes
Heat Input:	2.0 - 2.6 kJ/mm
	maintained by controlling run-out lengths (ROL)
Interpass Temperature:	230°C maximum

All welds were fully restrained using a purpose built jig. Backgouging by the carbon arc process was employed to remove strain-aged damage in the root region, prior to deposition of the final back passes. Details of the welding parameters are listed in Table 3. Figure 1 shows a typical pass sequence for the experimental welds. A hydrogen removal heat treatment (93°C for 24 h)

was performed on sections from each weldent used for tensile and crack-tip-opening-displacement (CTOD) specimens.

MECHANICAL TESTING

All weld-metal tensile specimens (6 mm dia.) were machined from each weld and tested. Charpy-V-notch (CVN) specimens were removed from the central portion (t/2 location) of each weldment transverse to the weld length. All specimens were notched through-thickness at the weld centreline. Transition curves were produced by testing over the temperature range of -70°C to +20°C in accordance with ISO standard R148-1960.

Full-thickness CTOD specimens removed from each weldment were notched through-thickness at the weld centreline. All specimens were locally compressed to 1% total strain for the ligament below the machined notch to facilitate the growth of straight fatigue cracks. Fatigue cracks were grown until a total crack length of 18-22 mm (a/w = 0.45 to 0.55) was reached. The tests were conducted at temperatures of -10°C and -30°C in accordance with British Standard BS5762:1979.

METALLOGRAPHY AND FRACTOGRAPHY

Full-thickness sections from each weld were prepared by standard metallographic techniques to facilitate measurements of the percentage of as-deposited and reheated weld metal regions. Optical microscopy was used to identify and characterize the weld metal microstructures. In addition, point counting was performed on the last as-deposited bead in accordance with the current IIW classification scheme (8). A total of 1000 points (50x20 grid) were evaluated in order to quantify the proportions of the following microstructural constituents; acicular ferrite (AF), grain boundary ferrite (GF), Ferrite with second phase (FS), and polygonal ferrite (PF).

Scanning electron microscopy (SEM) was employed to study the origins and modes of failure on fractured CVN and CTOD specimens.

RESULTS

Weld Metal Composition

Chemical compositions are given in Table 4 for the C-Mn welds and in Table 5 for the C-Mn-Ni welds. Carbon equivalents, which may be used to

relate hardenability to transformation behaviour were calculated for the compositions in Tables 4 and 5 and are given in Table 6 using the IIW formula (9), the P_{cm} formula (10) and Yurioka's CEN formula (11).

The core wires of the electrodes used for each weld were analyzed and their compositions are given in Table 7. In general there is little difference between electrodes in terms of core wire composition (approximately 0.07% C and 0.43% Mn). In general, additions of Mn, Si, Ni, Mo, Cr, Cu and Ti are made via the electrode coating. Elements such as S, P, Sn, Nb and V were picked-up from either the core wire or dilution of the parent plate, or both. Aluminum is not normally used as a deoxidant addition to these types of electrodes. The Al levels present in the base plate (Table 1) and electrode wires (Table 7) are higher than those in the weld deposits (<0.005%) since Al acts as a deoxidant during welding.

The chemical composition of the C-Mn weld deposits are given in Table 4. Ni, Mo, Cr, Cu and other elements are present in small quantities and come primarily from the dilution of the base material. The carbon levels of the welds are relatively similar ranging from 0.06% to 0.10% (0.07% average). Manganese varies between 1.25% and 1.55% with Si ranging from 0.34% to 0.68%. Manganese is generally used for its strengthening effect primarily by promoting the formation of acicular ferrite rather than solid solution hardening (12). Silicon is also used as a strengthening addition although it is primarily used as a deoxidant. The presence of silicon (usually above 0.2%) is also necessary for acceptable electrode operating characteristics and to prevent porosity. Too much Si, however, is detrimental to toughness (13) and the level is normally kept between 0.2% and 0.5%. For the C-Mn welds, oxygen varied from 211 ppm to 341 ppm with one weld, MA-20, at 471 ppm.

Ti, primarily from TiO in the coating, is also an important element with respect to producing desired acicular ferrite microstructures. The levels of Ti vary from less than 0.005% to 0.025%. One of the higher Ti weld metals, MA18, (0.02%) also contained 0.0009% Boron; all other welds had less than 0.0001%B.

In addition to Mn, Si and Ti; Ni and Mo are additions to the 1%, 2 1/2% and 3 1/2% Ni weld metals given in Table 5. Molybdenum is added primarily to increase strength. Its effects on toughness vary and only four of 12 electrodes studied contained molybdenum between 0.085% and 0.15%. Nickel additions are made to enhance both strength and low temperature toughness.

Nickel contents varied between 0.54% and 0.925% for the 1% Ni electrodes, 2.05% and 2.39% for the 2 1/2% Ni electrodes and 2.99% and 3.39% for the two 3 1/2% Ni electrodes. Oxygen contents for these welds varied between 291 ppm and 433 ppm.

MECHANICAL PROPERTIES

Tensile Properties

The tensile properties for the welds are shown in Table 8. All the C-Mn welds met the minimum tensile requirement of CSA Standard W48.1(14) (410 MPa yield, 500-650 MPa U.T.S. and 22% elongation). Requirements for the C-Mn-Ni welds are given in CSA Standard W48.3 (15). Welds MA-7, 12 and 16 (E55018-C3) met the requirements of 470-550 MPa minimum yield strength, 550 MPa minimum U.T.S. and 24% minimum elongation in the specified as-welded condition. The requirements for the remaining C-Mn-Ni welds are specified for the stress-relieved condition (minimum 450 MPa yield, 550 MPa U.T.S. and 19% elongation for E55018-C1 and C2 and minimum 390 MPa yield, 480 MPa U.T.S. and 25% elongation for E48016-C1L, E48018-G). A decrease in yield and ultimate strengths and an increase in elongation should occur between the as-welded and stress-relieved condition (16). Only the as-welded condition was examined and the tensile properties of these welds exceeded the requirements by a margin which should be large enough to compensate for any loss in strength due to stress relief.

Charpy Impact Tests

The Charpy impact results are shown as plots of impact energy vs test temperatures in Fig. 2 for the C-Mn welds and Fig. 3 for the C-Mn-Ni welds. Figures 2 and 3 are curves based on the average value of three tests per temperature.

For the C-Mn welds, Fig. 2, there is little difference between welds MA-3, 5 and 20. MA-13 has slightly poorer toughness than this group while MA-8 and 14 are shifted by 10 - 20°C to higher temperatures. MA-2 exhibited slightly better toughness than MA-3, 5 and 20 while MA-18 shows substantially higher toughness with over 50 J more upper shelf energy and a 40 J transition temperature of -57°C, 14°C lower than MA-2.

The C-Mn-Ni welds, Fig. 3, are grouped according to their nominal Ni content, 1%, 2 1/2% and 3 1/2%. Figure 3(a) shows the results for the 1% Ni welds. MA-1 has the highest toughness followed by MA-19. MA-12, MA-7 and MA-16. MA-1 has a substantially higher upper shelf and transition toughness compared with the others which is attributed to its lower yield and ultimate strengths since it is classed as an E48018-G. MA-16 shows the poorest lower shelf and transition toughness with an average 40 J temperature of approximately -25°C. The 2 1/2% Ni welds, Fig. 3(b), showed improved toughness compared with the 1% Ni welds with the lowest toughness weld, MA-15, exhibiting the same toughness as the second best 1% Ni weld, MA-19. MA-17 showed the best toughness of this group primarily due to its lower strength since it has an E48016-C1L classification compared with the E55018-C1 classification of the remaining electrodes. MA-4 has the best toughness of the E55018-C1 welds followed by MA-10, MA-6 and MA-15.

The Charpy toughness results for the two E55018-C2 welds, 3 1/2 Ni, are shown in Fig. 3(b). MA-9 shows the best toughness and is similar to MA-4 of the 2 1/2% Ni weld. MA-11 has the poorer toughness but is similar to MA-6 and is thus better than the poorest 2 1/2% Ni weld.

CTOD Tests

The results of the crack tip opening displacement (CTOD) tests are tabulated in Table 9 for the C-Mn welds, Table 10 for the C-Mn-1 Ni welds and Table 11 for the C-Mn-2 1/2 Ni and C-Mn-3 1/2 Ni welds. A minimum "required" CTOD can be derived using the proposed revisions to the U.K. Department of Energy's Guidance Notes for offshore structures by Pisarski and Harrison (17). For 20 mm thick welds in a region at high stress in the as-welded condition a CTOD of 0.08 mm is required for the surface breaking cracks which were assumed to be 10% of the weld thickness in depth for welds up to 50 mm thick. The 0.08 mm value applies to the minimum of three tests at a specific design/test temperature. In the current series of tests more than three tests were performed at a given test temperature (five at -30°C and four at -10°C). Hence a level higher than the lowest recorded test value may be used for acceptance purposes. This will be dealt with further in the discussion. However, several of the electrodes tested failed to achieve values greater than 0.08 mm at either test temperature while others were well above at -10°C and marginally above at -30°C.

For the C-Mn welds, MA-8, MA-13 and MA-14 were below the 0.08 value and gave δ_c values at both test temperatures. The majority of test results at both temperatures for MA-2, 5, 18 and 20 exceeded 0.08 mm whereas results for MA-3 were below 0.08 mm at -30°C and spread evenly above and below at -10°C.

The weld deposits of the 1% Ni containing electrodes generally resulted in values below 0.08 mm except for MA-1 tested at -10°C and MA-19 at both -30°C and -10°C. The 2 1/2 and 3 1/2 Ni welds generally showed the best fracture toughness in terms of CTOD although a considerable amount of scatter was observed. Welds MA-6 and 9 had the best overall toughness with all test values above 0.08 mm. Weld MA-15 had only one value below 0.08 mm, (at -30°C) while MA-10 and 11 had two values each below 0.08 mm (at -30°C). Weld MA-4 had one value at each of -30°C and -10°C below 0.08 mm while MA-17 showed the poorest toughness with three values below 0.08 mm at -30°C and one value below at -10°C.

MICROSTRUCTURE

In the vicinity of the CTOD crack front at the weld centreline the microstructure consisted of alternating layers of as-deposited (columnar), coarse-grain reheated and fine-grain reheated weld metal regions as shown, typically, in Fig. 4. The zone distributions are listed in Table 12. All welds contained at least 40% as-deposited weld metal for the full plate thickness, with the exception of weld MA-15 which had 36%. The central one-third and the CVN location (centre of weld) had higher amounts of reheated weld metal. In general the centre one-third had over 25% as-deposited structures with the exception of welds MA-10, 11, 15, 17 and 19. Welds MA-6, 15 and 17 were the only welds to have less than 25% as-deposited structure in the Charpy location. Observed variations in the distributions of as-deposited and reheated microstructures are a result of differences in operating characteristics of the different electrodes due to differences in electrode coating formulations.

It is well established that the microstructural constituents of a given weld depend on several important factors such as chemical composition, type and size distribution of non-metallic inclusions, austenite grain size and weld thermal cycle. Table 13 presents the results of the determination of the amounts of microstructural constituents in each weld measured by point

counting on the last as-deposited bead. As shown in the table, there is a wide variation in the amounts of various microstructural constituents. Representative microstructures are shown in Figs. 5 to 19. Typical microstructural constituents are indicated in Figs. 5 and 11.

Photo-micrographs showing as-deposited microstructures are presented in Figs. 5 to 9 for the C-Mn weld metals. The general microstructure consisted of an acicular ferrite matrix delineated by grain boundary ferrite and ferrite with second phase. The amount of acicular ferrite varied widely from 44% for MA-13 (Fig. 7) to 81% for MA-20 (Fig. 9) balanced by varying amounts of grain boundary ferrite and ferrite with second phase.

Photomicrographs of the C-Mn-1 Ni weld metals are shown in Figs. 10 to 13. In general the proportions of grain boundary ferrite and ferrite with second phase increased at the expense of acicular ferrite, although the austenite grain boundaries were less well defined compared to the C-Mn welds. Weld MA-19 was the exception with 69% acicular ferrite.

The C-Mn-2 1/2 Ni and C-Mn-3 1/2 Ni weld metal microstructures are shown in Figs. 14 to 19. The most notable features is an apparent reduction in austenite grain size and an increase, in general, in the amount of acicular ferrite compared with the 1% Ni weld metals.

Welds MA-1, MA-19 (1% Ni) and MA-17 (2 1/2% Ni) had significant variations in chemical composition compared with the electrodes within each group and thus do not necessarily follow the microstructural trends of the other weld metals in their respective groups.

The microstructures of the reheated regions are shown typically in Fig. 20. In general, the course-grain region consisted of equiaxed grains surrounded by grain boundary ferrite with an acicular ferrite matrix. The fine-grain regions consisted of polygonal ferrite and a carbide aggregate for all welds. In some cases, a carbide-rich structure decorated the grain boundaries in the C-Mn-Ni weld metals.

DISCUSSION

The results of the toughness tests for the twenty welds will be discussed to provide: a) a rating of electrodes relative to each other, b) an indication which features or combination of features promote good and poor toughness and c) an indication as to where improvements may be made or areas of research required to aid development of improved electrodes.

Toughness

The factors which influence the toughness of welded joints in C-Mn microalloyed structured steel have previously been reviewed by Braid and McGrath (18) and subsequently by Abson and Pargeter (19). Weld metal toughness is primarily controlled by two basic effects: microstructure and strain (18). The thickness of the plate and the welding procedure given in section 2.2 were chosen to minimize strain effects. The influence of residual stresses on fracture toughness increases with increasing plate thickness. Generally, welds in C-Mn microalloyed steel plates of thickness greater than 40-50 mm are stress relieved to remove residual stress for critical applications. The level of residual stresses in 20 mm thick plates, particularly after sectioning into Charpy and CTOD specimens, is expected to have a negligible effect on measured toughness although there is still enough of an effect to cause irregular fatigue crack shapes in CTOD specimens. This was observed for three specimens for weld MA-8, all other welds having undergone local compression to locally relieve the residual stresses.

Dynamic strain aging has been shown to contribute to the deterioration in toughness in the root regions of welded joints (20-22). The effects of dynamic strain aging on root toughness was minimized by fully restraining the test plates and by backgouging to remove strain-aged damaged material in the root region. Thus, variations in toughness between welds reflect the differences in electrode formulation and its effects on microstructure and inclusions.

CTOD Values for More Than Three Tests

Five CTOD tests were conducted at -30°C and four at -10°C for each weld. Normally, in defect assessments the current procedure is to use the lowest value of three tests at the service temperature of interest. When more than three tests are performed the probability of obtaining a value lower than the lowest of three tests increases as the number of tests increases. For more than three tests which value should one use in an evaluation? The lowest value, the next lowest or an average value? The values obtained from the tests represent samples from an unknown distribution. If enough samples were taken, say 50 to 100, then an average and standard deviation could be calculated which would be very close to the true mean and standard deviation. However, the costs involved in CTOD testing only permits a few tests to be

made. Since the tests represent a small, random sample then the probability exists that the majority of values in the sample set lie below the true mean. Hence, the use of the lowest of three test values. In this case the probability that the true mean is less than the minimum of three tests is 0.125 or 12.5%. As the sample size increases the probability that the true mean is less than the minimum value decreases. Since more than three tests have been performed at each temperature a value higher than the minimum of the test results might be used while maintaining the same risk as associated with the minimum of three tests. This can be evaluated using the Binomial Distribution. A more detailed discussion on this is presented in Appendix A. However, as shown in Table A-2 of Appendix A, six tests are required before the lowest value can be ignored and the next lowest used while maintaining the same, or lower risk as associated with using the minimum of three tests. Hence, for sample sizes of four and five tests the lowest values should be used (although the risk in using these values is lower than using the minimum of three tests).

Ranking of Weld Metals

The 40 J transition temperatures were determined from Figs. 2 and 3 and are given in Table 14. The welds are ranked in order of decreasing notch toughness using the 40 J transition temperatures and are given in Table 15. Also shown in Table 15 is a ranking, in order of decreasing fracture toughness, of the welds based on CTOD test results. As mentioned previously a minimum value of 0.08 mm is required for 20 mm thick joints in high stress regions in the as-welded condition. This was derived by Pisarski and Harrison (17), using the CTOD design curve, while developing the revisions to the U.K. Dept. of Energy Guidance Notes for offshore structures. The number of test values below 0.08 mm (at both -30°C and -10°C) for each weld were compared; the weld with the fewest values below 0.08 mm was judged to have the highest toughness. In the case of two welds having the same number of values below 0.08 mm, such as MA-2 and MA-5 (3 each), then the lowest value and highest values are considered. MA-2 was ranked higher than MA-5 since MA-2 had test values as high as 0.213 (-30°C) and 0.498 (-10°C) while MA-5 had values of 0.14 (-30°C) and 0.178 (-10°C). Also, the minimum values for MA-2 showed an improvement with increasing test temperature while MA-5 showed increased scatter and lower values when the test temperature was increased from -30°C to -10°C.

The welds were only compared against other welds in the same grouping, these being C-Mn, C-Mn-1 Ni, C-Mn-2 1/2 Ni and C-Mn-3 1/2 Ni. The C-Mn electrodes are all E480xx type while the C-Mn-Ni electrodes are primarily E550xx types (with the exception of MA-1 and MA-17) and the differences in strength, as well as Ni content (Ni increases the cleavage resistance of ferrite) contributes to the differences between the groups.

Comparison of the two rankings for the C-Mn welds indicates they are similar with two exceptions, MA-20 and MA-13. MA-13 changed from 6/8 based on CVN to 8/8 based on CTOD. The largest difference, however, is MA-20, ranked 5/8 based on CVN and 2/8 based on CTOD. There is little difference between the Charpy performance of MA-3, 5 and 20, however, the CTOD performance is substantially better and hence a better resistance to fracture initiation (although a large amount of scatter exists).

The rankings for the C-Mn-1 Ni welds are similar. The ranking of MA-1 ahead of MA-19 by CVN results reflects the strength difference of the two welds, E48018-G vs E55018-G. However, examination of Fig. 3(a) indicates that the 40 J temperatures are close and that MA-19 has a higher lower-shelf energy than MA-1. The CTOD performance of MA-19 is substantially better than all the other welds in the group. The E55018-C3 welds were consistently the poorest in this group.

The rankings for the C-Mn-2 1/2 Ni welds show opposite trends. In the case of the CVN based ranking, weld MA-10 had a marginally lower 40 J temperature than MA-4 (-64°C compared with -62°C). A difference of 2°C is within the scatter of the Charpy results recorded and MA-4 was judged to have better toughness since it maintained its upper shelf energy level to a lower temperature than MA-10 (See Fig. 3(b)). MA-17 has a higher upper shelf energy primarily due to its lower strength level (E48016-C1L). The large amount of scatter in the CTOD results made the ranking of toughness of the welds very difficult. MA-6 definitely had the highest minimum values at both test temperatures. However, differences between MA-4, 6 and 15 are not clear.

Both CVN and CTOD tests ranked MA-9 tougher than MA-11 for the C-Mn-3 1/2 Ni welds. These welds also showed comparable toughness values to the better welds of the C-Mn-2 1/2 Ni group.

Charpy vs CTOD

Anomalies and opposite trends in some of the rankings in the above section highlight the differences between Charpy and CTOD tests. Dawes (23)

has shown that it is not always possible to differentiate the toughness between welds using Charpy or sub-sized CTOD tests and it is necessary to test full-thickness specimens to determine clearly the fracture behaviour of a given weld. Apart from the higher constraint levels of full-thickness specimens, sub-sized specimens do not sample the full range of microstructures, inclusions and strain-affected regions. However, Charpy tests do give important information on dynamic effects and effects of blunt notches compared with the sharp cracks of CTOD specimens. Differences in toughness behaviour between Charpy and CTOD in AISI 4340 steels was rationalized by Ritchie et al. (24) by considering the location and distribution of cleavage crack initiation sites ahead of the notch or crack tip and the stress fields for a sharp crack (CTOD) and blunt notch (CVN). Gianetto and Braid (25) adapted this approach to explain differences in the toughness of two welds, one shielded metal arc and one submerged arc.

To understand the differences in measured toughness the micromechanisms of failure need to be determined.

FAILURE MECHANISMS

Several of the CTOD fracture surfaces were examined in the scanning electron microscope (SEM) to determine the origins and mode of fracture initiation. Failure, as shown in Fig. 21, occurs by cleavage, initiating at complex non-metallic oxy-sulfide inclusions. Initiation was also seen to occur primarily in as-deposited weld metal in grain boundary ferrite or ferrite with second phase microstructures. This is in agreement with the observations of Tweed and Knott (3). The size of initiating inclusions were observed to be greater than 1 μm. Also, the distance from the fatigue crack front to the initiating inclusion was seen to have an effect on the measured CTOD toughness. For weld MA-20 the initiating inclusion in the specimen showing low CTOD toughness (0.05 mm) was closer than that for the specimen showing high CTOD toughness (0.31 mm). For the CTOD specimen exhibiting good fracture toughness considerable ductile tearing occurred until the crack front reached the critical distance where the crack tip stresses caused cleavage initiation. Hence, the distribution of inclusions, > 1 μm diam, in the weld metal is one factor influencing the scatter in CTOD results.

All fractures in the CTOD tests originated in the centre 1/3 portion of the testpiece, the area of highest constraint. Table 12 indicates that the majority of the welds had 25% or more as-deposited microstructure in the centre 1/3 region. Five specimens, MA-10, 11, 15, 17 and 19, had between 25% and 10% as-deposited structure. Tweed and Knott (3) and Stout et al. (2) have demonstrated that reheated weld metal microstructures result in higher fracture toughness. The five welds with less than 25% as-deposited structure show a large scatter in CTOD results and had values less than 0.08 mm while welds with high amounts of as-deposited structure, such as MA-18 (51%), show good CTOD values. Hence, amounts of as-deposited structure as low as 10% along the crack front appear to be sufficient for fracture initiation. Thus microstructural constituents of as-deposited regions and non-metallic inclusion distributions appear to be more significant.

NON-METALLIC INCLUSIONS

The effects of non-metallic inclusions on ductile fracture are well known (see, for example, 26). This can be seen in the upper shelf Charpy energies when compared to the total oxygen and sulfur contents shown in Table 16. The higher upper shelf energies of MA-1 and MA-17 in their respective groups are due to their lower strength levels. The trends are clearly shown in the C-Mn-3 1/2 Ni weld, where MA-9 has higher upper shelf energy and lower O + S (0.0378%) compared with MA-11 (O+S = 0.0419%) as well as for some of the C-Mn welds where MA-18 has significantly higher upper shelf energy and the lowest O+S (0.0294%). Many of the welds have not reached their upper shelf energy levels at +20°C and would, if tested at higher temperatures, show the correct ordering with respect to O+S content. Differences in behaviour in the transition region are significantly affected by microstructure.

The size distributions of non-metallic inclusions were determined for some of the weld metals and are given in Table 17. Cross sections of the welds were polished to a 0.25 μm finish and inclusions were analysed using a Cambridge Instruments Quantimet 900 image analyser. The mean diameters of the inclusions were all less than 1.0 μm and the volume fractions of inclusions correspond to the O+S content of the weld metal (since oxygen has a very low solubility in iron). The distributions are seen to be skewed towards the smaller inclusion sizes.

Fracture initiation has been shown to occur at inclusions greater than 1 μm dia. Thus the tails of the distributions are important. Weld MA-14 has very poor CTOD toughness, and has a large number of large inclusions. Weld MA-5, also a C-Mn type, has a similar volume fraction of inclusions (and O+S level) to MA-14. However, MA-5 has fewer large inclusions (small tail of the distribution) and an improved CTOD performance. MA-18 has the lowest O+S of all the welds and hence a low volume fraction of inclusions. The size distribution for this weld shows a low number of large inclusions and good CTOD toughness. It is noted that MA-5, 14 and 18 have similar proportions of acicular ferrite. In a study on FCAW consumables, Bala and Santyr (1) also observed cleavage initiation from inclusions > 1 μm diam. However, the inclusion size distributions, performed using a scanning electron microscope , showed very few large inclusions. After analysis of a sample at CANMET, it was discovered that the area over which the counts on the FCA Welds had been performed was too small since inclusions less than 1 μm diam. dominate the distribution. Thus, it is necessary to ensure that a large enough field is used to properly characterize the tail of the distribution.

The make-up of the inclusions are complex oxy-sulfides containing deoxidant elements such as Al, Si, Ti and Mn as well as small amounts of Ni depending on the electrode. Some of the inclusions causing failure in weld MA-20 contained calcium and potassium, remanents of the electrode coating which become entrapped in the solidifying weld metal. The composition of inclusions will be discussed further during the discussion on microstructure.

The effects of inclusions on Charpy upper shelf energy has been discussed above. The failure mechanism in the lower shelf and lower transition regions is primarily cleavage. Gianetto and Braid (25) have studied two welds with relatively similar as-deposited microstructures. One weld had a large volume fraction of inclusions and a large number of inclusions > 1 μm dia. The other weld had a lower volume fraction of inclusions and a small number of inclusions > 1 μm dia. The low inclusion volume fraction weld showed good CTOD performance compared with the high inclusion volume fraction weld as was observed in the current programme. The Charpy results, however, were similar. This was explained using the model of Ritchie et al. (24) as shown in Figure 22. Since the average spacing of large, > 1 μm dia., inclusions was greater for the low volume fraction weld then the distance, ℓ, from the crack tip to the initiating inclusion is larger and hence a larger CTOD is

required for the stress, σ_{yy}, to become greater than the fracture stress, σ_F, at the initiating inclusion. However, the stress ahead of a round notch, as in the Charpy specimen, does not increase as rapidly as for a sharp crack and when the stress, σ_{yy}, ahead of the notch reaches the fracture stress, σ_F, initiation sites are available for both cases. Hence, although initiation of cleavage occurs at inclusions it is the critical fracture stress of the welds which control the lower shelf and transition region Charpy energies. Microstructure and weld metal chemistry thus have a significant effect on Charpy toughness since they control the critical fracture stress.

MICROSTRUCTURE

Resistance to cleavage fracture initiation is controlled by yield stress, ferrite grain (or colony) size, size and type of initiation nucleus and the resistance to cleavage of ferrite. Nickel, is known to enhance cleavage resistance of ferrite and this effect can be seen by comparing the lower shelf Charpy energies in Figs. 2 and 3. In general the welds with Ni additions, Fig. 3, (especially 2 1/2 & 3 1/2 Ni) have higher lower shelf energies than the C-Mn welds of Fig. 2. Silicon and nitrogen are known to have a deleterious effect (19). The largest effect, however, is that of microstructure and, in particular, grain size.

The improved toughness of reheated weld metal (2,3) is primarily a result of the formation of fine, equiaxed grains of ferrite. Garstone and Johnson (27) showed, for a series of SMAW deposits normalized using two different temperatures, that the toughness vs grain size data fitted a Hall-Petch type relationship. Grain boundaries and other high angle boundaries act as barriers to cleavage crack propagation. As the grain size decreases the unit crack length decreases and the energy for reinitiation in the next grain, and hence overall propagation, increases. Fractographic studies by Tweed and Knott (3) and McRobie and Knott (22) provide evidence that fine-grain material, in this case acicular ferrite, act as a barrier to crack propagation which was shown to preferentially follow grain boundary ferrite.

The grain size of both fine-grain and coarse-grain reheated weld metal are affected by heat input, welding position, preheat and interpass temperatures. These affect both the peak temperature and duration in the austenite temperature range which controls recrystallization and grain growth

(for a given weld chemistry, inclusion content, etc). These have been examined in detail by Evans (4,6,7). Toughness of E480xx and E550xx type weld metals generally decreases going from fine-grain reheated to coarse-grain reheated to as-deposited where long veins of grain boundary ferrite provide large unit crack lengths (3). As noted above acicular ferrite can act as a barrier to crack propagation in as-deposited weld metal due to its very small grain size. Hence, increased proportions of acicular ferrite should improve weld toughness.

The microstructures of the welds are compared with Charpy toughness in Table 18 and CTOD in Table 19. Welds MA-1 and MA-17 have been omitted from the 1% Ni and 2 1/2% Ni groups respectively owing to their lower strength levels. Table 18 shows in general, with a few notable exceptions, that Charpy toughness increases with increasing amounts of acicular ferrite and decreasing amounts of grain boundary ferrite. The exceptions are MA-14 and MA-20 for the C-Mn welds and MA-15 for the C-Mn-2 1/2 Ni welds. Although MA-20 has the highest proportion of acicular ferrite and lowest amount of grain boundary ferrite it also has the highest O+S level providing more possible cleavage crack initiation sites. MA-14 has a low amount of grain boundary ferrite, average O+S, and a high amount of acicular ferrite. However, MA-14 has a high silicon level (0.68 wt%) which is known to reduce the cleavage resistance of ferrite (19) and promote poor toughness (13). For the C-Mn-2 1/2 Ni welds MA-15 has a higher acicular ferrite and lower grain boundary ferrite than MA-6 and 10. Also, it has a higher amount of reheated weld metal than the other C-Mn-2 1/2 Ni welds and average O+S level. Examination of the chemistry (Table 5) of MA-15 reveals a higher carbon level which results in a higher hardenability (CE, Table 6), although the tensile properties are similar to the other C-Mn-2 1/2 Ni welds. The reason for the poorer Charpy performance may be related to the martensite-austenite phase located between the acicular ferrite laths. Further investigation of this is required.

Table 19 shows, with two exceptions, that good CTOD toughness is related to large amounts of acicular ferrite and low amounts of grain boundary ferrite. As with the Charpy-microstructure comparisons above, weld MA-14 shows poor CTOD performance despite a high amount of acicular ferrite. This has been linked to a large number of inclusions > 1μm dia. and to a high amount of silicon which lowers the cleavage resistance of ferrite. Weld MA-6 has a low amount of acicular ferrite and a high O+S content, yet produced the

best CTOD results. It is suspected that this weld has a low number of inclusions >1 μm, however, further analysis is required.

The above comparisons confirm that increasing the proportion of acicular ferrite and decreasing grain boundary ferrite promotes increased toughness. A review of the compositions given in Tables 4 and 5 associated with high amounts of acicular ferrite and high toughness reveals, for C-Mn welds, an optimum composition of 0.08%C, 1.4% Mn and 0.35% Si in close agreement with the works of Evans (12,13,28), Widgery (29) and others (19). Nickel is generally added to increase strength and the cleavage resistance of ferrite. Taylor and Evans (30) have shown that nickel also refines the acicular ferrite but does not necessarily increase the amount of acicular ferrite. The highest amount of acicular ferrite produced for the nickel bearing consumables tested was for weld MA-19 at 69%. In general manganese is decreased to between 1.0% and 1.3% when nickel is added. Higher manganese contents cause the formation of martensite and hence loss of toughness particularly at the 3.5% nickel level (30, 31).

Four of the nickel-containing welds had additions of approximately 0.1% molybdenum. Small additions of Mo, up to 0.1%, have been reported to reduce grain-boundary ferrite and increase the proportion of acicular ferrite (31). The welds with the Mo additions had acicular ferrite contents of 50% or more and manganese levels close to 1.0%.

Tables 4 and 5 indicate that most of the welds contain between 0.010 and 0.030% titanium with MA-18 containing ~0.001% boron. Titanium and/or boron have been shown to increase the proportion of acicular ferrite. Titanium affects the size distribution and composition of non-metallic inclusions, in the size range 0.25-0.75 μm, which act as nucleation sites for acicular ferrite (32-35). The combination of titanium and boron inhibits the formation of grain boundary ferrite and reduces free nitrogen (36), further improving toughness. The titanium and boron (for MA-18) levels are within the optimum ranges for these elements quoted by Masumoto (37) as 0.01 - 0.05% for titanium and 0.001-0.003% for boron (this may vary depending on nitrogen pickup).

As noted above, the presence of oxide inclusions in the size range 0.25 - 0.75 μm act as the nucleation sites for acicular ferrite formation. From Tables 4 and 5 oxygen levels vary from 211 ppm to 471 ppm. The C-Mn welds with the highest proportions of acicular ferrite, MA-18 and 20 (77% & 81%) have oxygen contents of 234 ppm and 471 ppm respectively. MA-18 benefits from a small addition of boron, however, comparison with MA-2, 5 and 14

(73%, 68% and 72% acicular ferrite respectively) indicates that oxygen levels down to 200 ppm are sufficient to nucleate high proportions of acicular ferrite. Higher levels, above 450 ppm, are thought to pin austenite grain boundaries (32) resulting in observed smaller austenite grain sizes in high oxygen containing welds. The finer austenite grain size provides a larger grain boundary area for ferrite nucleation promoting observed increases in proportions of grain boundary ferrite. Too low an oxygen content does not provide sufficient nuclei for acicular ferrite also resulting in poor toughness microstructures of grain boundary ferrite and ferrite with second phase.

Composition and shape may be important for the ability of inclusions to nucleate acicular ferrite. Shape may be important when considering match or mismatch between crystallographic planes in the inclusions and in ferrite (34,35,38,39). Other work has indicated that inclusion chemistry is important with Ti (32-35,) and Al (40) containing inclusions promoting acicular ferrite. Effects of inclusion shape and chemistry were not investigated in the present study owing to their complexity. However, further improvements in weld-metal toughness will require a detailed study on inclusion shape and composition.

CONCLUSIONS

Test results on 20 shielded-metal-arc welding electrodes of the C-Mn and C-Mn-Ni types indicate that few of the C-Mn electrodes meet toughness requirements for -30°C design temperatures while approximately half would meet requirements for -10°C. The addition of nickel, in amounts of 2.5% to 3.5% improves toughness such that there are potentially four electrodes of the E55018-C1 and C2 types which could meet requirements for -30°C. The following conclusions are made based on the evaluation of test results.

Low temperature fracture occurred by cleavage initiation from large, >1 μm dia., inclusions primarily located in grain boundary ferrite of as-deposited weld metal. Poor CTOD toughness was associated with welds containing large numbers of inclusions, >1 μm diameter. CTOD toughness for welds of similar microstructure and inclusion volume fraction improved when the number of large inclusions were reduced.

Improved toughness is associated with small grain size. In as-deposited weld metal this is associated with a high proportion of acicular ferrite microstructure. For C-Mn weld metals, high amounts of acicular ferrite and good toughness were associated with weld metal chemistries of 0.08%C,

1.4% Mn, 0.35% Si, 0.02% Ti and oxygen between 200 and 400 ppm. The addition of 0.001% boron in weld MA-18 was seen to have a beneficial effect on toughness and microstructure. The C-Mn-1 Ni welds generally showed poor toughness, particularly for the E55018-C3 electrodes, as a result of as-deposited microstructures consisting of high proportions of grain boundary ferrite and ferrite with second phase. The C-Mn-2.5 Ni and C-Mn-3.5 Ni welds showed improved low temperature toughness owing to the increase in cleavage resistance of ferrite and a refinement of acicular ferrite. These welds also showed increased scatter in CTOD test values indicating a problem with large inclusions. In general the microstructure of the C-Mn-Ni weld metals did not have as high an amount of acicular ferrite as did the C-Mn welds.

A high level of Si, >0.5%, was responsible for the poor toughness of one of the C-Mn welds. Although the weld had a high proportion of acicular ferrite the high Si level caused a decrease in the cleavage resistance of the ferrite.

FUTURE WORK

Several areas have been indicated where further work may result in improvements in toughness and microstructure of shielded-metal-arc welds for use in C-Mn microalloyed structural steel.

1. Further optimization of electrode coatings to reduce or eliminate large inclusions > 1 μm dia.

2. Further optimization of titanium and boron additions to increase the proportions of acicular ferrite. An understanding of the role of nitrogen in determining optimum levels is also required.

3. Previous work has shown that inclusions in the size range 0.25 to 0.75 μm dia. act as acicular ferrite nucleation sites. The optimum oxygen levels to form these inclusions appear to lie between 200 ppm and 400 ppm although low levels are preferred to improve upper shelf toughness. Hence, the mechanism by which inclusions act as acicular ferrite nucleation sites and the roles of inclusion shape and composition need to be determined.

4. Optimization of chemical composition and size distribution of inclusions is required for C-Mn-Ni weld metals to reduce scatter in CTOD results and increase proportions of acicular ferrite. The increased cleavage resistance of ferrite with Ni combined with improvements in reducing large inclusions and increasing acicular ferrite should result in welds suitable for use at -50°C.

REFERENCES

1. Bala, S.R. and Santyr, S., Final Report for DSS/CANMET Contact OSQ 84-00080 by AMCA Int'l. Kanata, March, 1986.

2. Stout, R.D., McLaughlin, P.F. and Strunk, S.S., Weld J., Vol. 48 No. 4, 1969. pp 155s-160s.

3. Tweed, J.H. and Knott, J.F., Met. Sci., Vol. 17, No. 2, 1983. pp 45-54.

4. Evans, G.M., Weld Res. Abroad, Vol. 29, No. 1, 1983. pp 24-35.

5. Evans, G.M. Weld Res. Abroad, Vol. 29, No. 1, 1983. pp 35-45.

6. Evans, G.M., Weld Res Abroad, Vol. 29, No.1, 1983. pp 46-57.

7. Evans, G.M., Weld Res. Abroad, Vol. 29, No. 1, 1983. pp 58-69.

8. Pargetter, R.J. and Dolby, R.E., IIW Doc. No IXJ-102-85, 1985.

9. Technical Report - Commission IX of IIW, IIW Doc. No. IX-535-67, 1967.

10. Ito, Y and Bessyo, K., Journal Jap. Weld Soc., Vol. 37, No. 9, 1968. pp 983-991.

11. Yurioka, N., Suzuki, H. Ohshita, S. and Saito, S., Weld J., Vol. 62, No. 6, 1983. pp 147s-153s.

12. Evans, G.M., Weld Res. Abroad, Vol. 29, No. 1, 1983. pp 2-12.

13. Evans, G.M., Met. Const., Vol. 18, No. 7, 1986. pp 438R - 444R.

14. CSA Standard W48.1 - M1980, Mild Steel Covered Arc Welding Electrodes, Canadian Standards Association, Toronto, 1980.

15. CSA Standard W48.3 - M1982, Low Alloy Steel Covered Arc Welding Electrodes, Canadian Standards Association, Toronto, 1982.

16. Braid, J.E.M. and Gianetto, J.A., in Welding for Challenging Environments, Proc. Int. Conf., Toronto, Pergamon Press, Toronto, 1986. pp 145-155.

17. Pisarski, H.G. and Harrison, J.D., in Welding for Challenging Environments, Proc. Int. Conf., Toronto, Pergamon Press, Toronto, 1986. pp 131-144.

18. Braid, J.E.M. and McGrath, J.T., Can. Met. Quart., Vol. 25, No. 2, 1986. pp 131-143.

19. Abson, D.J. and Pargeter, R.J., Int. Met. Rev., Vol. 13, No. 4, 1986.

20. Cochrane, R.C., Terry, P., and Garland, J.G., Weld and Met. Fab., Vol. 44, No. 4 and 6, 1976. pp 316-320,439-448.

21. Berkhaut, C.F. and Van den Brink, S.H., Weld and Met. Fab., Vol. 46, No. 5, 1978. pp 347-351.

22. McRobie, D.E. and Knott, J.F., Met. Sci and Tech., Vol. 1, 1985. pp 357-365.

23. Dawes, M.G., Weld and Met. Fab., Vol. 40, No. 3, 1972. pp 95-104.

24. Ritchie, R.O., Francis, B. and Server, W.L., Met. Trans., Vol. 7A, No. 6, 1976. pp 831-838

25. Gianetto, J.A. and Braid, J.E.M., Division Report PMRL 85-71 (TR), CANMET, Energy, Mines and Resources Canada, 1985.

26. Knott, J.F., "Fundamentals of Fracture", Butterworths, London, 1973.

27. Garstone, J. and Johnson, F.A., Br. Weld J., Vol. 10, No. 5, 1963. pp 224-230.

28. Evans, G.M., Weld Res. Abroad, Vol. 29, No. 1, 1983. pp. 13-24.

29. Widgery, D.J., Research Report M/27/68, British Welding Research Association, 1968.

30. Taylor, D.S. and Evans, G.M., Met. Const., Vol. 15, No. 8, 1983. pp 438-443.

31. Judson, P. and McKeown, D., Proc. 2nd. Int. Conf. Offshore Welded Structures, Weld Inst., London, 1982. Paper 3.

32. Cochrane, R.C. and Kirkwood, P.R., Proc. Int. Conf. Trends in Steels and Consumables for Welding, Weld. Inst. London, 1978.

33. Harrison, P.L. and Farrar, R.A., J. Mat. Sci., Vol. 16, 1981. pp 2218-2226.

34. Ricks, R.A., Howell, P.R. and Barritte, G.S., J. Mat. Sci., Vol. 17, 1982. pp. 732-740.

35. Kayali, E.S., Corbett, J.M. and Kerr, H.W., J. Met. Sci. Let., Vol. 2, 1983. pp 123-128.

36. Tsuboi, J. and Terashima, J., Welding in the World, Vol.12, No. 11/12, 1983. pp 304-316.

37. Masumoto, I., IIW. Doc. No. XII-694-79, 1979.

38. Cochrane, R.C. and Keville, B.R., Proc. Conf. Steel for Linepipe and Pipeline Fittings, Weld. Inst., London, 1981. pp 51-60.

39. Keville, B.R., Weld, J., Vol. 62, No. 9, 1983. pp 253s - 260s.

40. Bhatti, A.R., Saggese, M.E., Hawkins, D.N., Whiteman, J.A. and Golding, M.S., Weld, J., Vol. 63, No. 7, 1984. pp 224s - 230s.

Table 1 - Chemical composition of 350 WT base material

Base Material	Element wt %								
	C	Mn	Si	S	P	Al	Ni	V	Nb
350 WT	0.15	1.44	0.24	0.005	0.015	0.015	0.225	0.060	0.020

Table 2 - Electrode Type and Principal Alloy

Principal Alloy	Electrode Type (CSA)	Weld Identification
C-Mn	E48018-1	MA-2
	E48016-1	MA-3
	E48018-1	MA-5
	E48018	MA-8
	E48018-1	MA-13
	E48018	MA-14
	E48016-1	MA-18
	E48018-1	MA-20
C-Mn-1Ni	E48018-G	MA-1
	E55018-C3	MA-7
	E55018-C3	MA-12
	E55018-C3	MA-16
	E55018-G	MA-19
C-Mn-2 1/2Ni	E55018-C1	MA-4
	E55018-C1	MA-6
	E55018-C1	MA-10
	E55018-C1	MA-15
	E48016-C1L	MA-17
C-Mn-3 1/2Ni	E55018-C2	MA-9
	E55018-C2	MA-11

Table 3 Welding parameters for SMA welds

Side No.	Pass No.	Current (Amps)	Voltage (Volts)	Travel Speed (mm/s)	Heat Input (KJ/mm)
1	1	110	19	6.3	2.0
	2	130	19	5.7	2.6
	3	130	19	5.7	2.6
	5	110	19	6.3	2.0
	6	110	19	6.3	2.0
2	4	130	19	5.7	2.6

Table 4 - Chemical Composition of C-Mn Weld Metals

Weld	Element (wt%)											(ppm)	
	C	Mn	Si	S	P	Ni	Cr	Sn	Cu	V	Ti	N	O
MA-2	0.07	1.38	0.505	0.008	0.015	0.090	0.025	0.010	0.105	<0.005	0.025	132	313
MA-3	0.10	1.38	0.495	0.004	0.015	0.090	0.025	0.010	0.105	<0.005	0.025	123	211
MA-5	0.06	1.53	0.470	0.010	0.015	0.070	0.015	0.002	0.002	0.010	0.005	93	341
MA-8	0.06	1.25	0.520	0.014	0.014	0.050	0.020	0.005	0.010	0.005	0.015	132	296
MA-13	0.06	1.34	0.485	0.009	0.014	0.065	0.020	0.007	0.010	0.010	0.007	165	333
MA-14	0.09	1.31	0.680	0.010	0.015	0.080	0.025	0.006	0.010	0.015	0.015	116	319
MA-18	0.07	1.55	0.340	0.006	0.010	0.060	0.030	0.005	0.020	<0.005	0.020	78	234
MA-20	0.08	1.44	0.390	0.007	0.013	0.060	0.015	0.005	0.005	0.015	<0.005	101	471

Note: Nb $\leq$0.005, Mo <0.01, Al $\leq$ 0.005

MA18 contained 0.0009% Boron

Table 5 - Chemical Composition of C-Mn-Ni Weld Metals

Weld	Element (wt%)												(ppm)	
	C	Mn	Si	S	P	Ni	Cr	Mo	Sn	Cu	V	Ti	N	O
C-Mn-1Ni														
MA-1	0.08	1.42	0.380	0.005	0.014	0.925	0.025	<0.010	0.005	0.010	0.030	0.010	53	336
MA7	0.08	1.11	0.485	0.011	0.014	0.885	0.020	0.085	0.006	0.030	0.010	0.008	138	315
MA12	0.06	1.01	0.520	0.013	0.020	0.850	0.025	0.100	0.005	0.015	0.010	0.015	99	364
MA16	0.08	0.77	0.365	0.013	0.014	0.855	0.045	<0.010	0.005	0.010	<0.010	0.010	118	430
MA19	0.08	1.45	0.310	0.011	0.015	0.540	0.060	<0.010	0.010	0.125	0.015	<0.005	130	433
C-Mn-2 1/2Ni														
MA4	0.06	1.13	0.430	0.007	0.013	2.39	0.020	0.014	0.002	0.025	0.020	0.020	76	351
MA6	0.05	1.30	0.445	0.016	0.013	2.24	0.02	<0.010	0.004	0.035	0.010	0.008	81	387
MA10	0.05	1.02	0.410	0.010	0.011	2.08	0.020	0.150	0.005	0.015	0.010	0.010	135	291
MA15	0.10	1.29	0.460	0.010	0.014	2.07	0.040	<0.010	<0.005	0.005	0.015	0.010	116	358
MA17	0.06	0.75	0.400	0.007	0.017	2.05	0.020	<0.010	0.005	0.020	<0.005	0.030	151	348
C-Mn-3 1/2Ni														
MA9	0.06	0.85	0.310	0.008	0.015	3.39	0.035	<0.010	0.005	0.040	0.015	0.020	129	298
MA11	0.07	1.15	0.390	0.010	0.016	2.99	0.040	0.150	0.005	0.025	0.010	0.010	163	319

Note: Nb $\leq$ 0.005, Al $\leq$ 0.005

Table 6 - Calculated Carbon Equivalents for Weld Metals

Weld	CE_{IIW}	Pcm	CEN
C-Mn			
MA-2	.318	.164	.220
-3	.348	.194	.275
-5	.325	.155	.214
-8	.277	.143	.189
-13	.294	.147	.197
-14	.322	.183	.250
-18	.340	.167	.231
-20	.330	.169	.235
C-Mn-1Ni			
MA-1	.390	.184	.261
-7	.349	.176	.240
-12	.313	.152	.201
-16	.275	.148	.194
-19	.381	.164	.258
C-Mn-2 1/2Ni			
MA-4	.420	.176	.243
-6	.424	.157	.238
-10	.396	.162	.224
-15	.464	.218	.329
-17	.327	.147	.195
C-Mn-3 1/2Ni			
MA-9	.440	.175	.243
-11	.503	.205	.293

Table 7 - Chemical Composition of SMAW Core Wires

Name	Electrode Type(CSA)	Element								
		C	Mn	Si	S	P	Al	Cu	Ni	Cr
MA-1	E48018-G	0.068	0.530	<.005	0.0094	0.0053	0.04	0.010	0.025	0.010
-2	E48018-1	0.071	0.490	0.005	0.015	0.012	0.10	0.035	0.025	0.010
-3	E48016-1	0.083	0.475	0.005	0.011	0.0072	0.10	0.135	0.054	0.010
-4	E55018-C1	0.063	0.490	0.090	0.013	0.010	0.06	0.025	0.040	0.010
-5	E48018-1	0.055	0.455	<.005	0.011	0.0063	0.08	0.020	0.030	0.015
-6	E55018-C1	0.057	0.410	"	0.021	0.005	0.02	0.010	0.015	0.015
-7	E55018-C3	0.075	0.480	"	0.014	0.0058	0.09	0.010	0.025	0.010
-8	E48018	0.029	0.325	"	0.012	0.007	0.03	0.055	0.030	0.015
-9	E55018-C2	0.085	0.470	"	0.021	0.010	0.10	<.005	0.015	0.020
-10	E55018-C1	0.086	0.505	"	0.010	0.0038	0.06	0.020	0.025	0.015
-11	E55018-C2	0.095	0.450	"	0.017	0.0081	0.10	0.010	0.015	0.015
-12	E55018-C3	0.081	0.470	"	0.019	0.0087	0.13	0.025	0.020	0.015
-13	E48018-1	0.056	0.285	"	0.014	0.0054	0.04	<.005	0.015	0.010
-14	E48018	0.085	0.370	"	0.016	0.0046	0.10	0.010	0.010	0.010
-15	E55018-C1	0.13	0.400	"	0.011	0.0052	0.10	<.005	0.005	0.010
-16	E55018-C3	0.072	0.325	"	0.019	0.0025	0.10	0.005	0.010	0.010
-17	E48016-C1	0.030	0.305	"	0.011	0.014	0.07	0.020	0.030	0.015
-18	E48016-1	0.031	0.325	"	0.011	0.0071	0.07	0.025	0.025	0.015
-19	E55018-G	0.068	0.525	"	0.017	0.0069	0.10	0.130	0.070	0.065
-20	E48018-1	0.070	0.500	"	0.0075	0.0047	0.05	0.005	0.020	0.010

For all Wires: V <.005
Ti <.005
Nb <.005
Mo <.010
Sn <.005

Table 8 - Tensile Properties

Weld No.	Yield Strength (MPa)	Ultimate Strength (MPa)	Elongation in 4 dia. (%)	Reduction of Area (%)
C-Mn				
MA-2	517	624	28	72
MA-3	490	622	29	72
MA-5	465	572	31	75
MA-8	499	585	26	71
MA-13	494	584	31	76
MA-14	520	620	27	70
MA-18	486	528	28	73
MA-20	539	647	25	69
C-Mn-1Ni				
MA-1	521	616	28	69
MA-7	507	608	27	71
MA-12	516	616	26	68
MA-16	486	569	27	70
MA-19	553	647	27	69
C-Mn-2½ Ni				
MA-4	574	680	24	70
MA-6	525	637	24	69
MA-10	576	664	26	69
MA-15	572	670	26	71
MA-17	470	583	33	75
C-Mn3½ Ni				
MA-9	572	656	28	72
MA-11	638	729	26	69

Table 9 - CTOD Results for C-Mn Weld Metals

Test Temperature	MA-2	MA-3	MA-5	MA-8	MA-13	MA-14	MA-18	MA-20
-30°C	0.084(u)	0.061(c)	0.140(u)	-	0.018(c)	0.030(c)	0.130(u)	0.130(u)
	0.061(c)	0.010(c)	0.140(u)	-	0.025(c)	0.060(c)	0.190(u)	0.050(u)
	0.213(u)	0.069(u)	0.110(u)	0.086(u)	0.030(c)	0.060(c)	0.130(u)	0.310(u)
	0.046(c)	0.109(u)	0.074(u)	0.030(c)	0.018(c)	0.020(c)	0.239(u)	0.058(u)
	0.081(u)	0.056(c)	0.102(u)	0.015(c)	0.033(c)	0.018(c)	0.074(u)	0.175(u)
-10°C	0.064(c)	0.036(c)	0.178(u)	-	0.023(c)	0.013(c)	0.264(u)	0.211(u)
	0.229(u)	0.180(u)	0.071(u)	0.048(c)	0.041(c)	0.061(c)	0.145(u)	0.457(u)
	0.498(m)	0.020(c)	0.157(u)	0.056(c)	0.043(c)	0.036(c)	0.312(u)	0.137(u)
	0.338(u)	0.236(u)	0.030(c)	0.079(u)	0.018(c)	0.033(c)	0.173(u)	0.257(u)

CTOD - mm, Fracture Type: (c)-δc, (u) - δu and (m) - δm

Table 10 - CTOD Results for C-Mn-1Ni Weld Metals

Test Temperature	MA-1	MA-7	MA-12	MA-16	MA-19
-30°C	0.041 (c)	0.050 (c)	0.060 (c)	0.010 (u)	0.183 (u)
	0.079 (u)	0.030 (c)	0.020 (c)	0.099 (u)	0.109 (u)
	0.041 (c)	0.040 (c)	0.020 (c)	0.013 (c)	0.226 (u)
	0.064 (c)	0.023 (c)	0.015 (c)	0.043 (c)	0.130 (u)
	0.020 (c)	0.041 (c)	0.036 (c)	0.053 (c)	0.043 (c)
-10°C	0.140 (u)	0.030 (c)	0.033 (c)	0.056 (c)	0.470 (m)
	0.109 (u)	0.056 (c)	0.114 (u)	0.020 (c)	0.175 (u)
	0.155 (u)	0.046 (c)	0.023 (c)	0.064 (c)	0.394 (m)
	0.145 (u)	0.041 (c)	0.033 (c)	0.023 (c)	0.122 (u)

CTOD - mm, Fracture Type: (c)-δc, (u)-δu and (m)-δm

Table 11 - CTOD Results for C-Mn-2½ Ni and C-Mn-3½ Ni Weld Metals

Test Temperature	C-Mn-2½ Ni					C-Mn-3½ Ni	
	MA-4	MA-6	MA-10	MA-15	MA-17	MA-9	MA-11
-30°C	0.167 (u)	0.160 (u)	0.064 (c)	0.305 (u)	0.036 (c)	0.130 (u)	0.140 (u)
	0.340 (u)	0.160 (u)	0.086 (u)	0.241 (u)	0.100 (u)	0.120 (u)	0.160 (u)
	0.050 (u)	0.200 (u)	0.099 (u)	0.036 (c)	0.140 (u)	0.130 (u)	0.050 (c)
	0.292 (u)	0.152 (c)	0.127 (u)	0.229 (u)	0.013 (c)	0.084 (u)	0.163 (u)
	0.221 (u)	0.114 (u)	0.043 (c)	0.112 (u)	0.018 (c)	0.112 (u)	0.074 (c)
-10°C	0.064 (u)	0.320 (m)	0.099 (u)	0.351 (m)	0.127 (u)	0.371 (u)	0.272 (u)
	0.241 (u)	0.142 (u)	0.160 (u)	0.351 (m)	0.163 (u)	0.122 (u)	0.363 (m)
	0.173 (u)	0.470 (m)	0.399 (u)	0.122 (u)	0.033 (c)	0.107 (u)	0.269 (m)
	0.528 (u)	0.203 (u)	0.231 (u)	0.446 (m)	0.472 (u)	0.279 (u)	0.300 (m)

CTOD - mm, Fracture Type: (c) - δc, (u)-δu and (m) - δm

Table 12 - Distribution of As-deposited (columnar), and Reheated Weld Metal Regions Along the Weld Centreline

Weld No.	Full Plate Thickness (%)		Central One-Third (%)		CVN Location (%)	
	A	(R)	A	(R)	A	(R)
C-Mn						
MA-2	56	(44)	34	(66)	44	(56)
MA-3	51	(49)	26	(74)	35	(65)
MA-5	51	(49)	37	(63)	31	(69)
MA-8	51	(49)	31	(69)	47	(53)
MA-13	40	(60)	29	(71)	42	(58)
MA-14	62	(38)	50	(50)	44	(56)
MA-18	56	(44)	51	(49)	45	(55)
MA-20	57	(43)	30	(70)	51	(49)
C-Mn-1Ni						
MA-1	52	(48)	25	(75)	41	(59)
MA-7	55	(45)	28	(72)	31	(69)
MA-12	44	(56)	25	(75)	32	(68)
MA-16	44	(56)	28	(72)	31	(69)
MA-19	51	(49)	17	(83)	27	(73)
C-Mn-2½ Ni						
MA-4	46	(54)	26	(74)	30	(70)
MA-6	50	(50)	30	(70)	22	(78)
MA-10	50	(50)	22	(78)	28	(72)
MA-15	36	(64)	19	(81)	16	(84)
MA-17	41	(59)	10	(90)	13	(87)
C-Mn-3½ Ni						
MA-9	52	(48)	28	(72)	37	(63)
MA-11	42	(58)	13	(87)	26	(74)

A - As-deposited, R - Reheated

Table 13 - Microstructural Constituents of As-deposited Weld Metals

Weld No.	% of Constituent				
	AF	GF	FS(A)	FS(N)	PF
C-Mn					
MA-2	73	12	4	7	4
MA-3	48	25	11	13	4
MA-5	68	17	5	6	4
MA-8	49	23	11	11	6
MA-13	44	26	10	12	8
MA-14	72	9	8	7	4
MA-18	77	11	4	5	3
MA-20	81	9	4	3	3
C-Mn-1Ni					
MA-1	49	23	10	14	4
MA-7	30	16	20	27	7
MA-12	50	19	7	15	9
MA-16	31	31	15	18	5
MA-19	69	12	7	10	2
C-Mn-2½ Ni					
MA-4	67	13	7	8	5
MA-6	40	20	12	21	7
MA-10	55	10	15	14	6
MA-15	60	10	15	10	5
MA-17	50	18	19	10	3
C-Mn-3½ Ni					
MA-9	52	19	13	12	4
MA-11	50	10	20	12	8

AF - Acicular Ferrite

GF - Grain Boundary Ferrite

FS(A) - Ferrite with Second Phase (aligned)

FS(N) - Ferrite with Second Phase (non-aligned)

PF - Polygonal Ferrite

Table 14 - 40J Charpy Transition Temperatures

Weld Number	40J Temperature (°C)
C-Mn	
MA-2	-43
MA-3	-37
MA-5	-39
MA-8	-23
MA-13	-30
MA-14	-19
MA-18	-57
MA-20	-38
C-Mn-1Ni	
MA-1	-51
MA-7	-31
MA-12	-37
MA-16	-24
MA-19	-47
C-Mn-2½ Ni	
MA-4	-62
MA-6	-52
MA-10	-64
MA-15	-46
MA-17	-59
C-Mn-3½ Ni	
MA-9	-58
MA-11	-50

Table 15 - Ranking of Toughness of Weld Metals

- based on 40J Charpy transition temperature and the number of CTOD test values above/below 0.08mm. Ranking in order of decreasing toughness.

Weld Type	Ranking Based on CVN	Ranking Based on CTOD
C-Mn	MA-18	MA-18
	-2	-20
	-5	-2
	-3	-5
	-20	-3
	-13	-8
	-8	-14
	-14	-13
C-Mn-1Ni	MA-1	MA-19
	-19	-1
	-12	-12
	-7	-7
	-16	-16
C-Mn-2½ Ni	MA-4	MA-6
	-10	-15
	-17	-4
	-6	-10
	-15	-17
C-Mn-3½ Ni	MA-9	MA-9
	-11	-11

Table 16 - Oxygen + Sulphur

Weld	O+S
C-Mn	
MA-2	0.0393
-3	0.0251
-5	0.0441
-8	0.0436
-13	0.0423
-14	0.0419
-18	0.0294
-20	0.0541
C-Mn-1Ni	
MA-1	0.0386
-7	0.0425
-12	0.0494
-16	0.0560
-19	0.0543
C-Mn-2½ Ni	
MA-4	0.0421
-6	0.0547
-10	0.0391
-15	0.0458
-17	0.0418
C-Mn-3½ Ni	
MA-9	0.0378
-11	0.0419

Table 17 - Non-metallic Inclusion Size Distributions

Weld	Volume Fraction	Mean Size (μm)	Number of Inclusions per Unit Area*					No/mm^2	O+S
			0-1 μm	1-2 μm	2-3 μm	3-4 μm	4-5 μm	>1 μm	
C-Mn									
MA-5	0.38	0.86	16226	1483	33	1	0	92.44	.044
MA-14	0.35	0.87	15086	1538	69	13	1	98.84	.042
MA-18	0.26	0.90	9789	1338	30	1	0	83.55	.029
C-Mn-1Ni									
MA-12	0.33	0.88	11634	1281	13	1	0	101.04	.049
C-Mn-21/2Ni									
MA-4	0.43	0.88	10109	1057	16	0	1	65.45	.042
C-Mn-31/2Ni									
MA-9	0.23	0.94	6668	1734	37	8	0	108.41	.038

* Unit Area = 16.41mm^2

Table 18 - Comparison of Charpy Toughness and Microstructure

Weld*	%AF	%GF	%A	O+S
C-Mn				
MA-18	77	11	45	.029
-2	73	12	44	.039
-5	68	17	31	.044
-3	48	25	35	.025
-20	81	9	51	.054
-13	44	26	42	.042
-8	49	23	47	.044
-14	72	9	44	.042
C-Mn-1Ni				
MA-19	69	12	27	.054
-12	50	19	32	.049
-7	30	16	31	.043
-16	31	31	31	.056
C-Mn-2½ Ni				
MA-4	67	13	30	.042
-10	55	10	28	.039
-6	40	20	22	.055
-15	60	10	16	.046
C-Mn-3½ Ni				
MA-9	52	19	37	.038
-11	50	10	26	.042

* Welds in order of decreasing Charpy toughness.

AF - Acicular Ferrite, GF - Grain Boundary Ferrite

%A - %As-deposited Structure O+S - Oxygen + Sulphur

Table 19 - Comparison of CTOD and Microstructure

Weld*	%AF	%GF	%A†	O+S
C-Mn				
MA-18	77	11	51	.029
-20	81	9	30	.054
-2	73	12	34	.039
-5	68	17	37	.044
-3	48	25	26	.025
-8	49	23	31	.044
-14	72	9	50	.042
-13	44	26	29	.042
C-Mn-1Ni				
MA-19	69	12	17	.054
-12	50	19	25	.049
-7	30	16	28	.043
-16	31	31	28	.056
C-Mn-2½ Ni				
MA-6	40	20	30	.055
-15	60	10	19	.046
-4	67	13	26	.042
-10	55	10	22	.039
C-Mn-3½ Ni				
MA-9	52	19	28	.038
-11	50	10	13	.042

* Welds in order of decreasing CTOD

AF - Acicular Ferrite, GF - Grain Boundary Ferrite, O+S - Oxygen + Sulphur

†%A - % As-deposited structure in centre 1/3 of CTOD test piece.

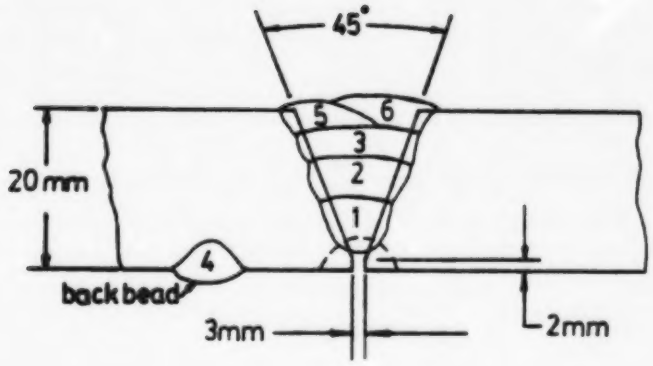

Fig. 1 Typical pass sequence for experimental welds (neg.15497).

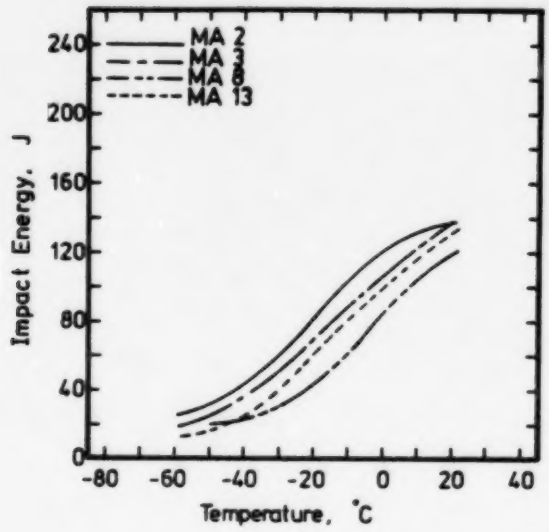

(a) (neg. 15476)

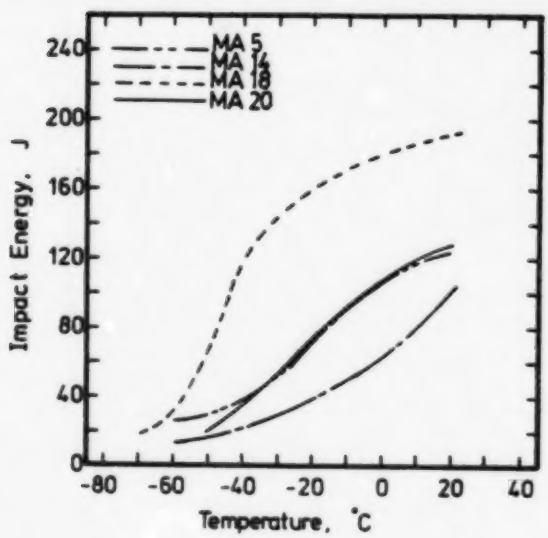

(b) (neg. 15475).

Fig. 2 Charpy impact transition curves for C-Mn welds.

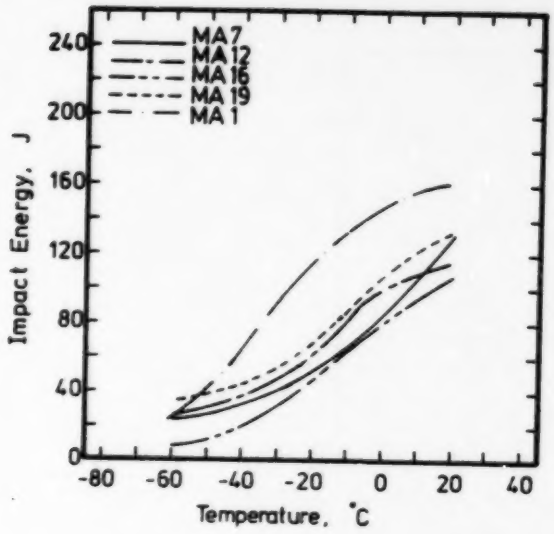

(a) 1% Ni (neg.15484)

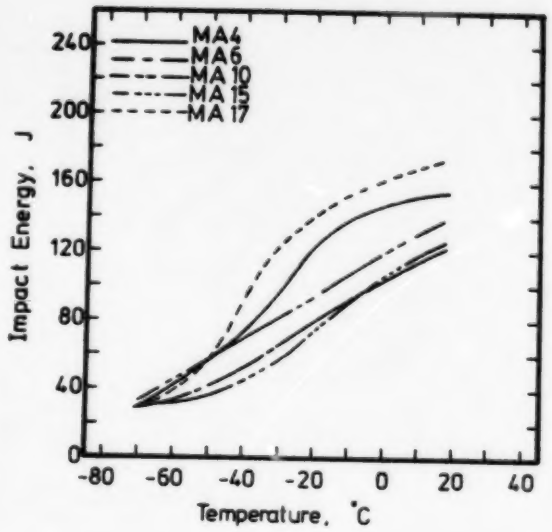

(b) 2 1/2 % Ni (neg.15474)

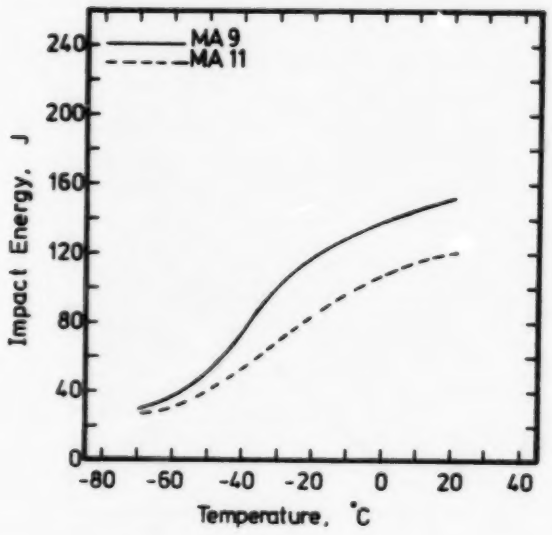

(c) 3 1/2 % Ni (neg.15473)

Fig. 3 Charpy impact transition curves for C-Mn-Ni welds.

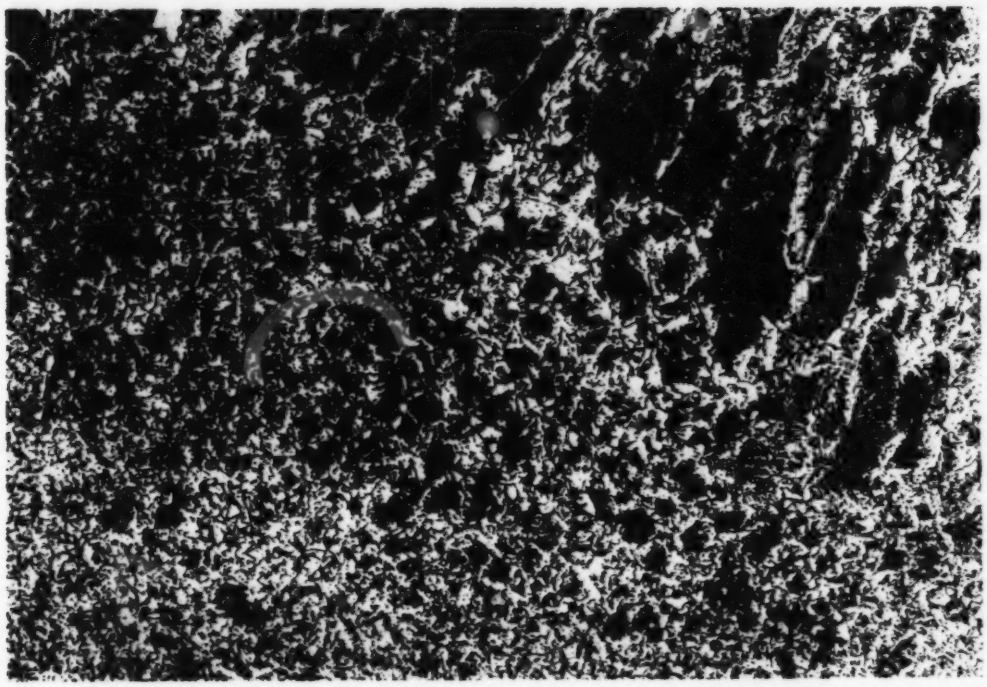

Fig. 4 Microstructural regions at weld centerline consisting of as-deposited (columnar), coarse grain and fine grain reheated structures. (neg.17490).

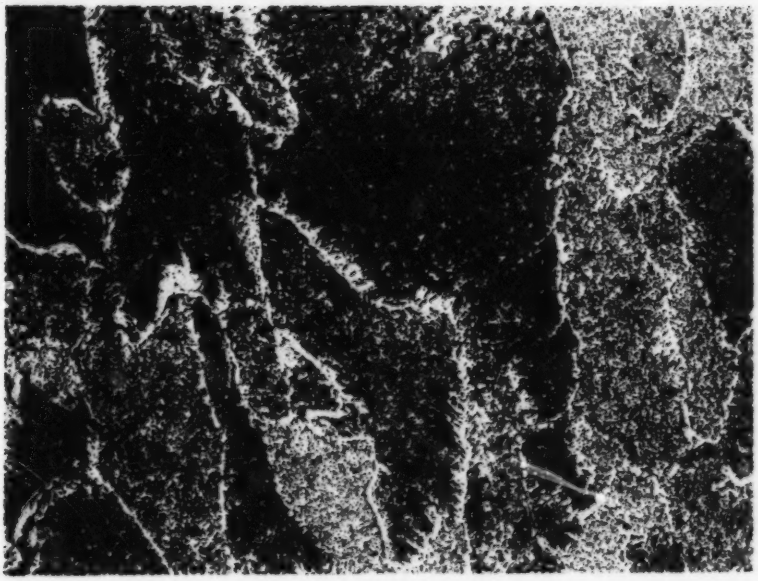

(a) (neg.17491)

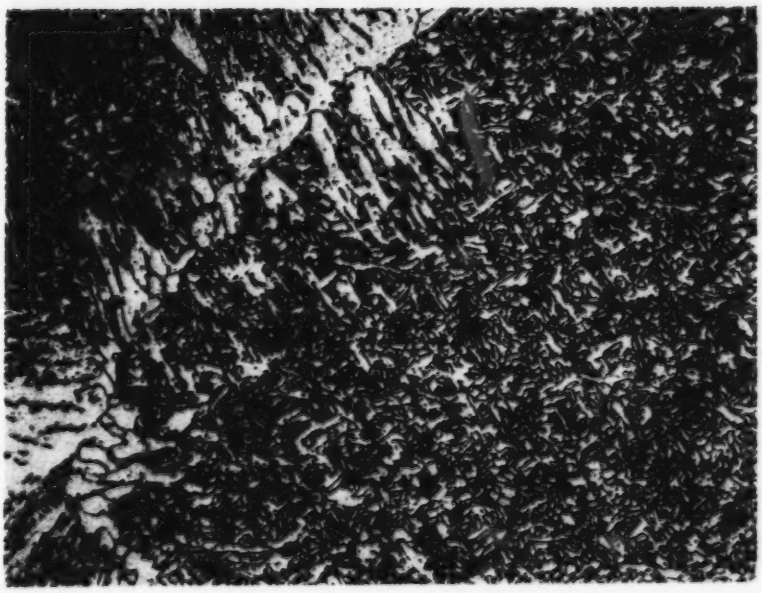

(b) (neg.17492)

Fig. 5 Microstructure of weld MA-5 showing microstructural constituents: AF-Acicular Ferrite, GF-Grain Boundary Ferrite, FS(A)-Ferrite with second phase (aligned), FS(N)-Ferrite with second phase (nonaligned), PF-Polygonal Ferrite, Etch: 2% Nital.

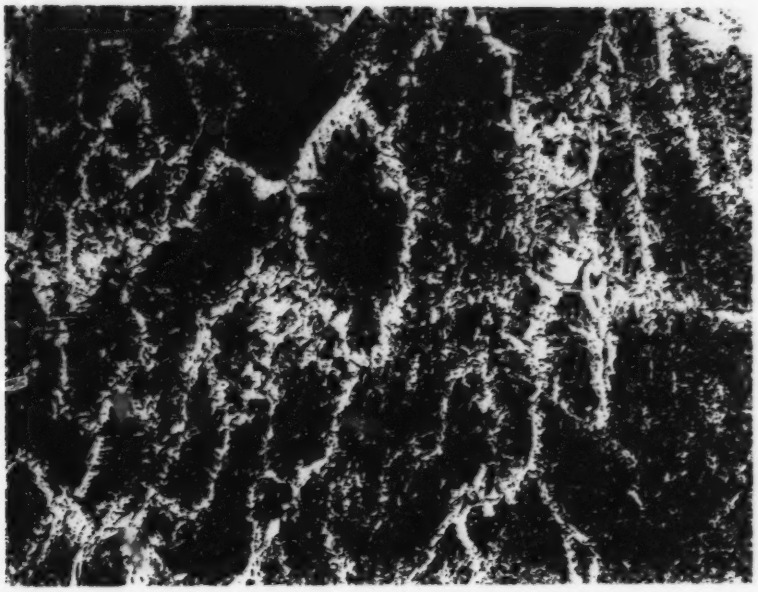

(a) (neg.17493)

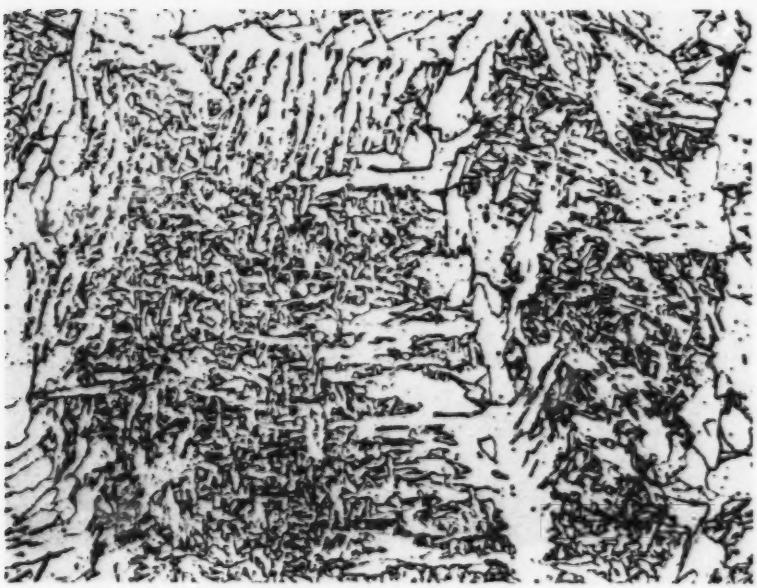

(b) (neg.17494)

Fig. 6 Microstructure of weld MA-8. Etch 2% Nital.

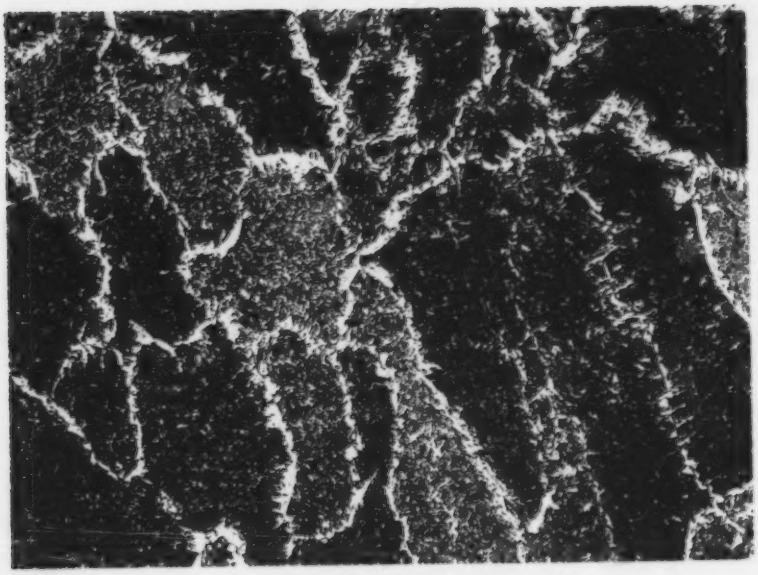

(a) (neg.17495)

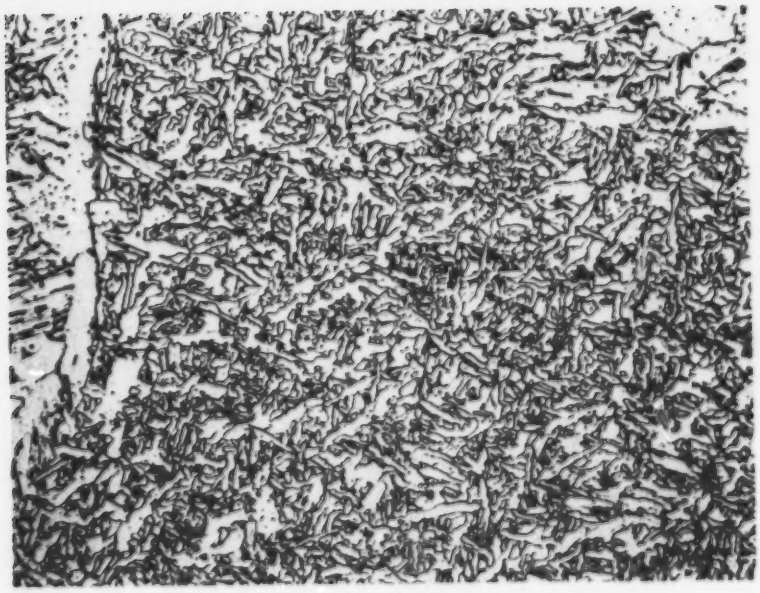

(b) (neg.17496)

Fig. 7 Microstructure of weld MA-13. Etch 2% Nital.

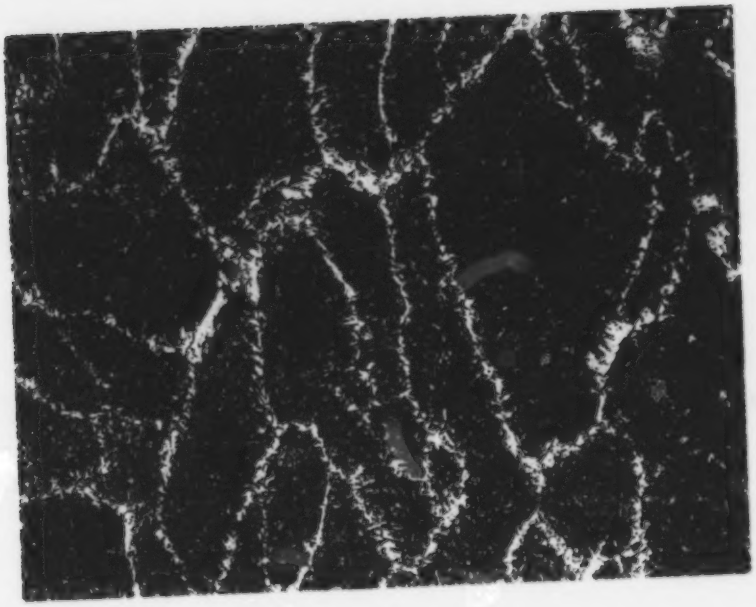

(a) (neg.17497)

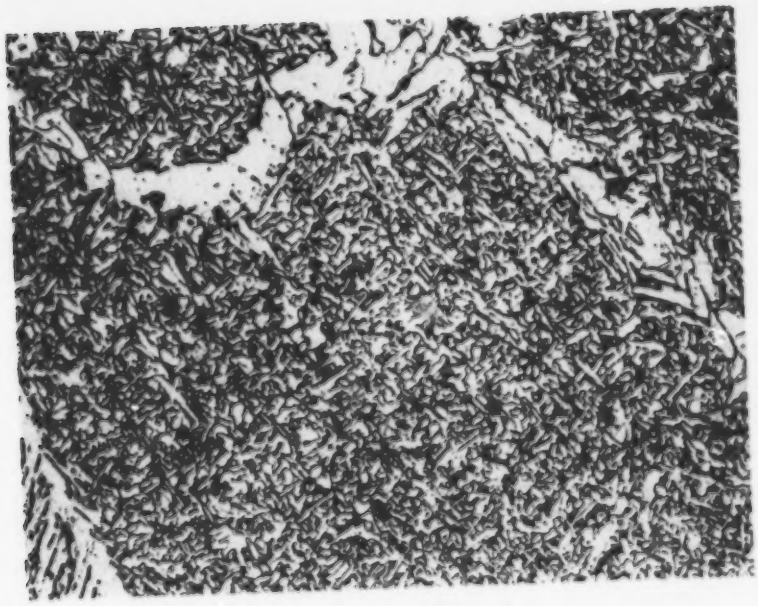

(b) (neg.17498)

Fig. 8 Microstructure of weld MA-18. Etch 2% Nital.

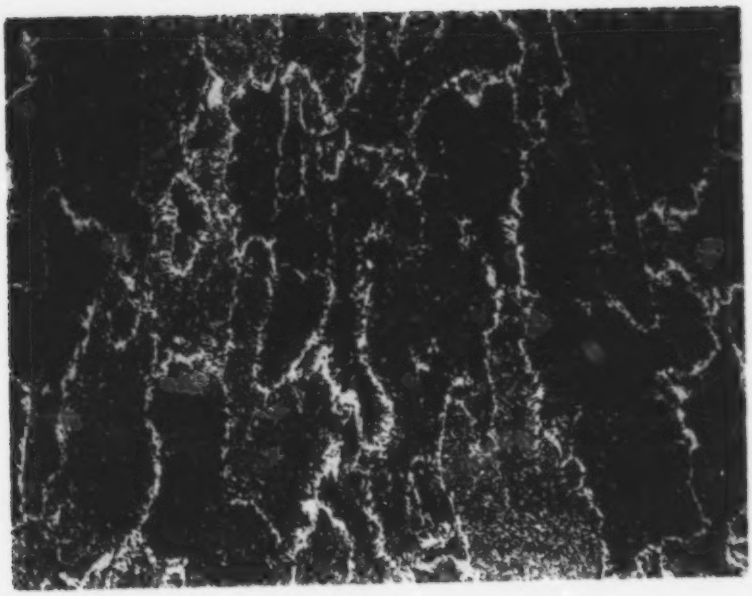

(a) (neg.17499)

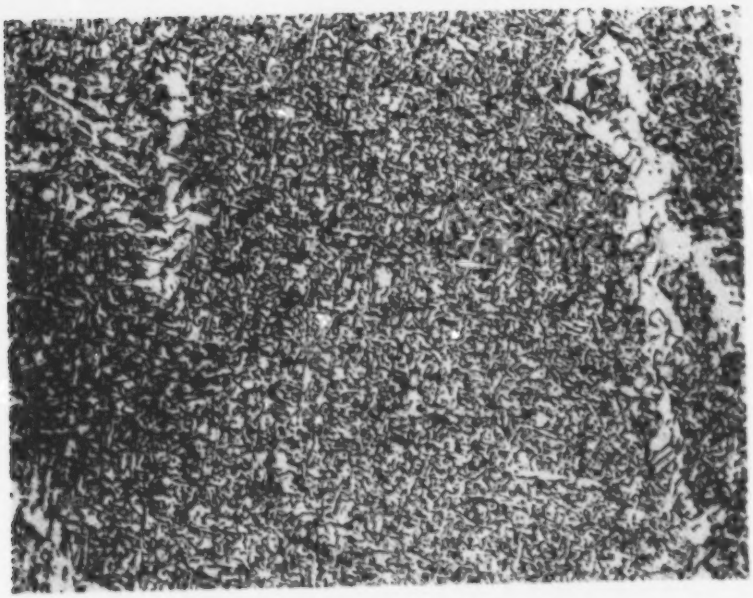

(b) (neg.17500)

Fig. 9 Microstructure of weld MA-20. Etch 2% Nital.

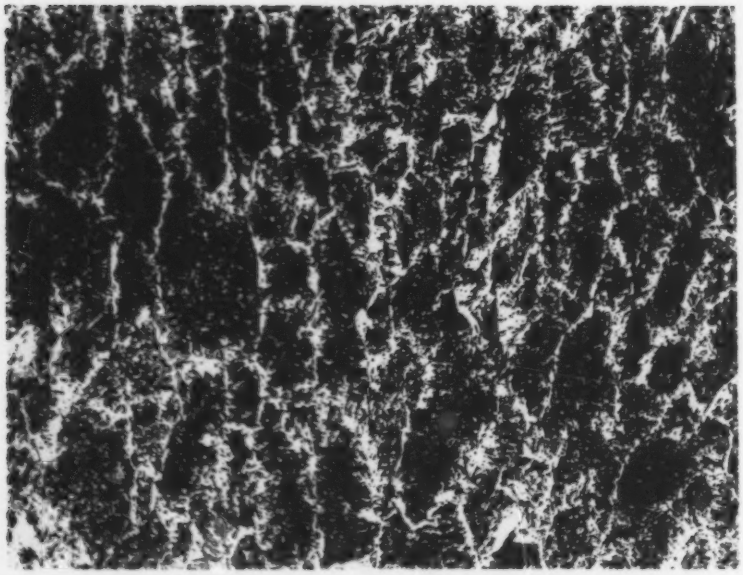

(a) (neg.17501)

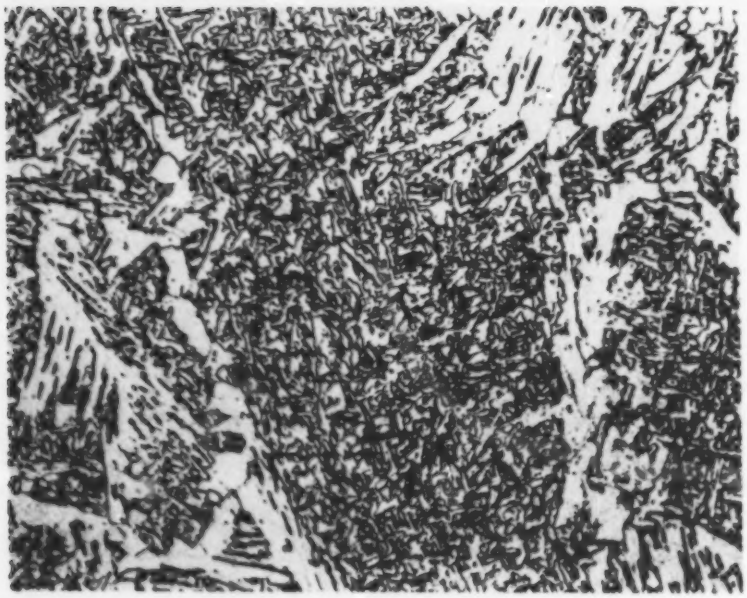

(b) (neg.17502)

Fig. 10 Microstructure of weld MA-1. Etch 2% Nital.

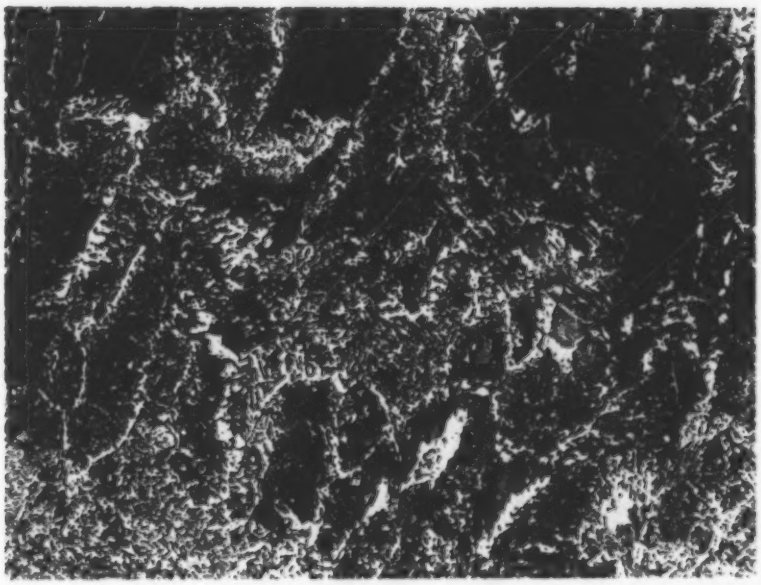

(a) (neg.17503)

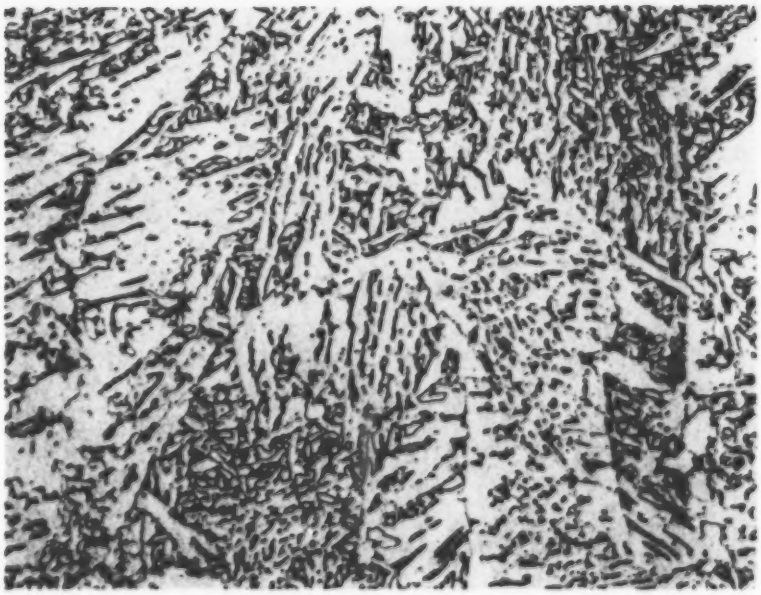

(b) (neg.17504)

Fig. 11 Microstructure of weld MA-7. Etch 2% Nital.

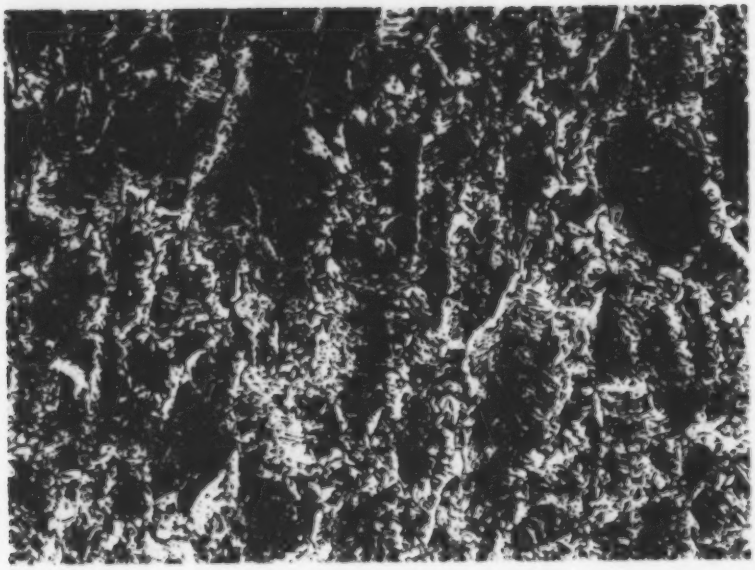

(a) (neg.17505)

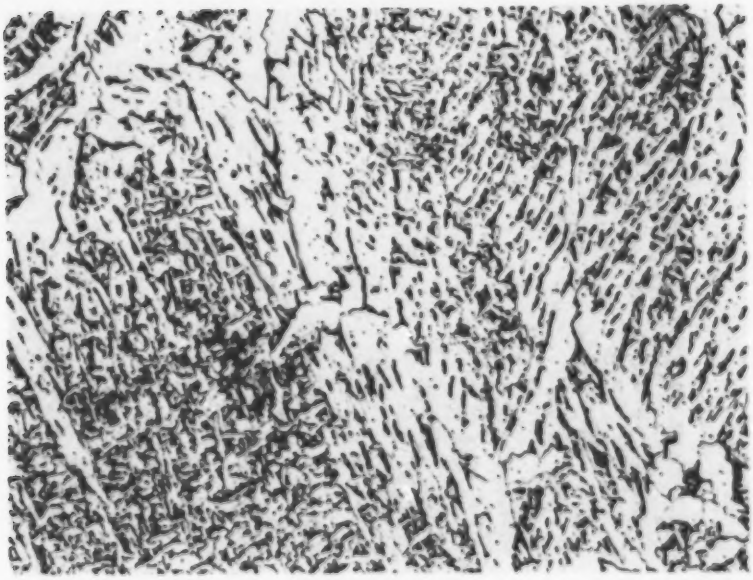

(b) (neg.17506)

Fig. 12 Microstructure of weld MA-16. Etch 2% Nital.

(a) (neg.17507)

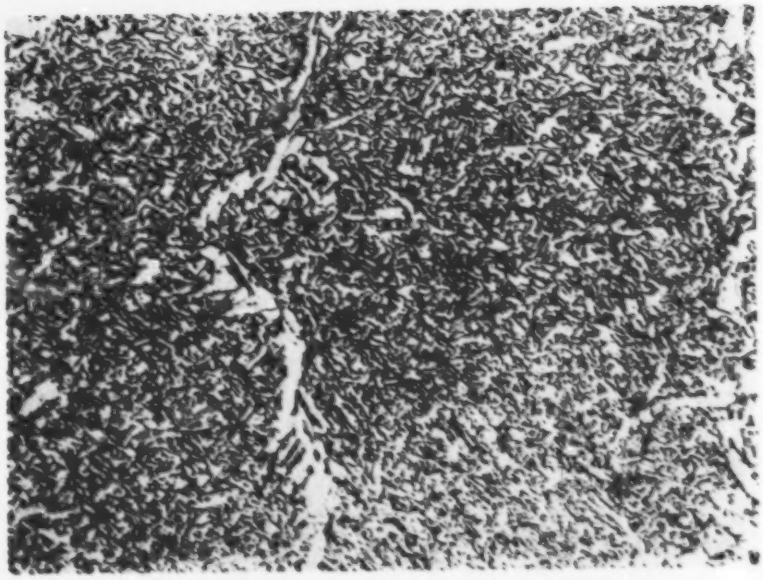

(b) (neg.17509)

Fig. 13 Microstructure of weld MA-19. Etch 2% Nital.

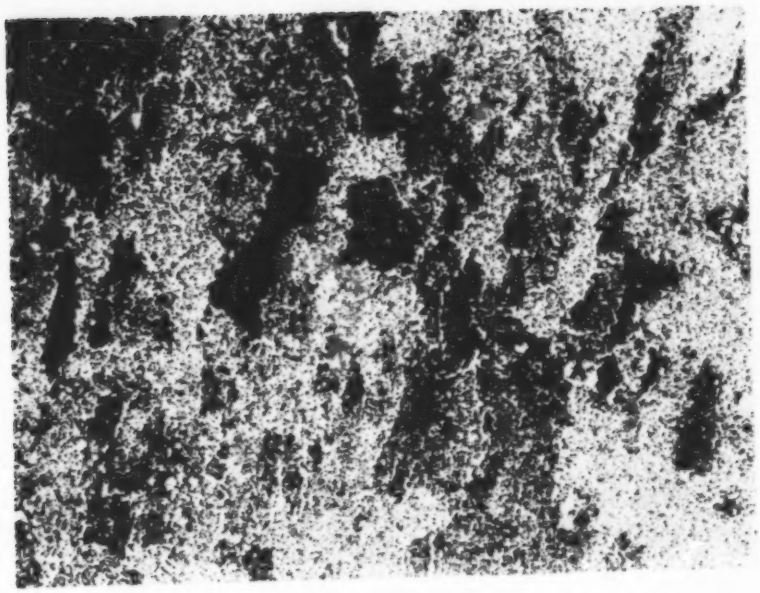

(a) (neg.17510)

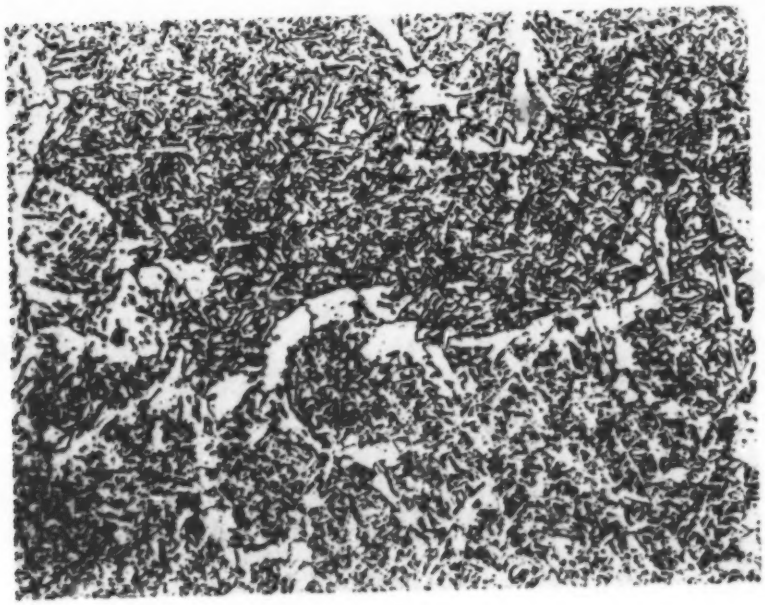

(b) (neg.17511)

Fig. 14 Microstructure of weld MA-4. Etch 2% Nital.

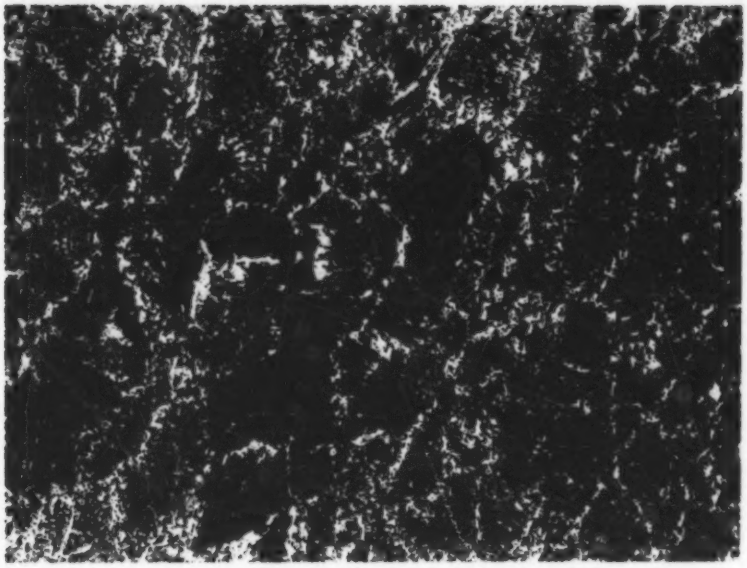

(a) (neg.17512)

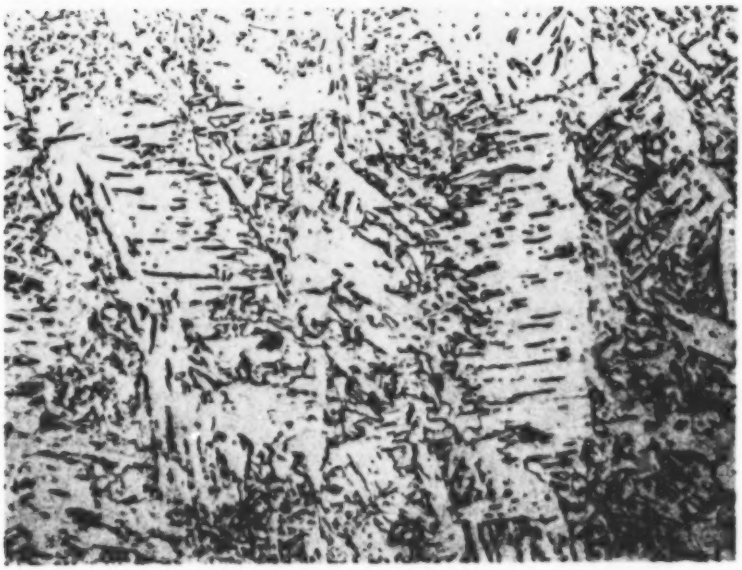

(b) (neg.17513)

Fig. 15 Microstructure of weld MA-6. Etch 2% Nital.

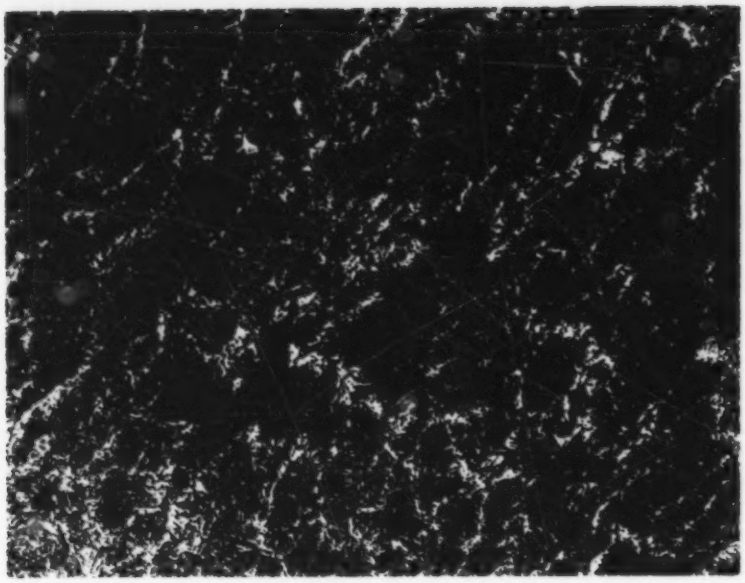

(a) (neg.17514)

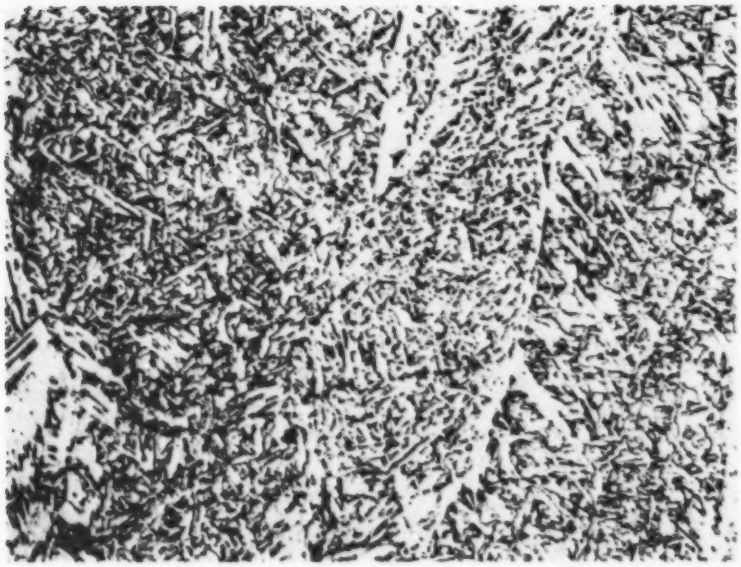

(b) (neg.17515)

Fig. 16 Microstructure of weld MA-10. Etch 2% Nital.

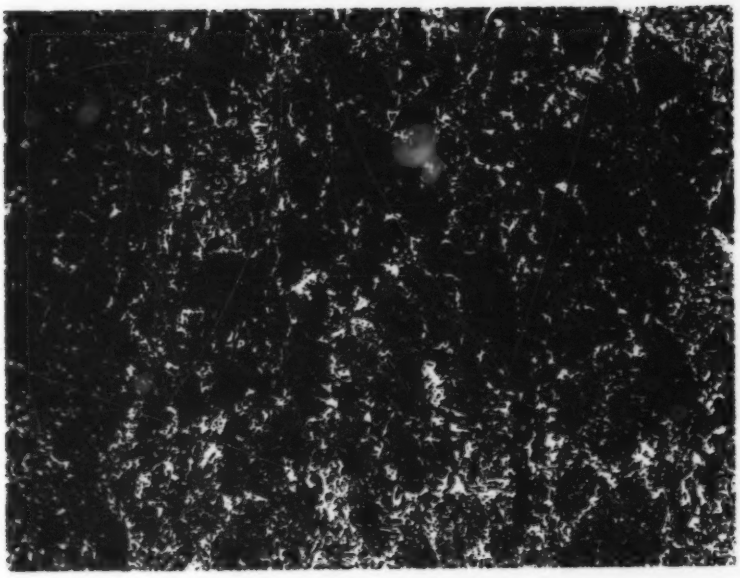

(a) (neg.17516)

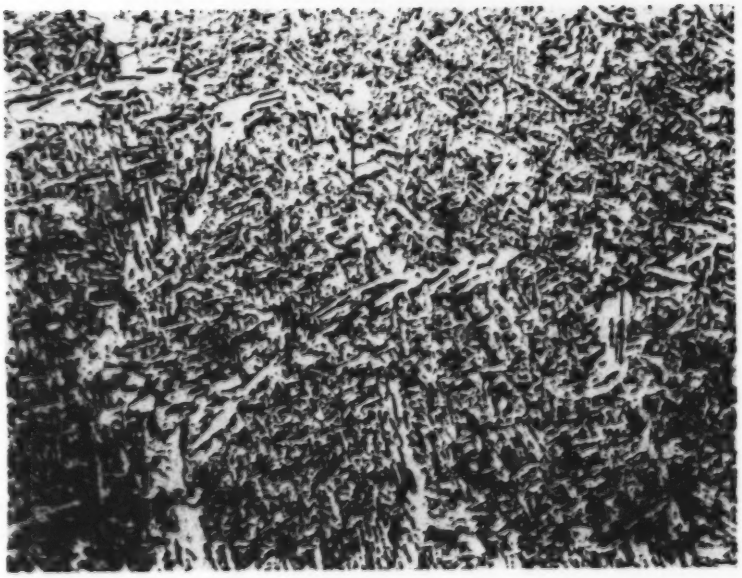

(b) (neg.17517)

Fig. 17 Microstructure of weld MA-15. Etch 2% Nital.

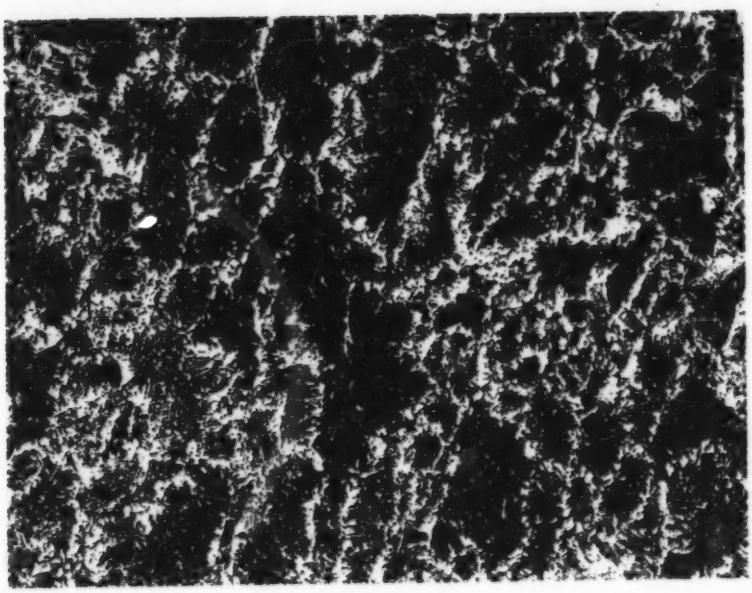

(a) (neg.17518)

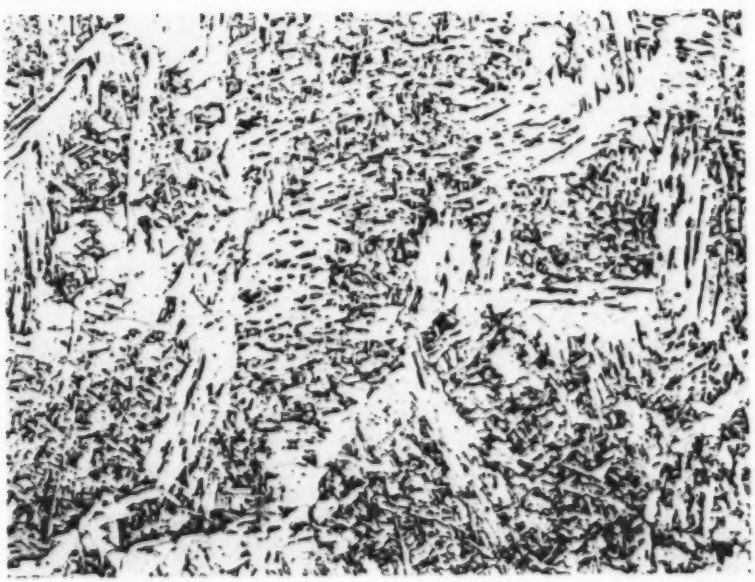

(b) (neg.17519)

Fig. 18 Microstructure of weld MA-17. Etch 2% Nital.

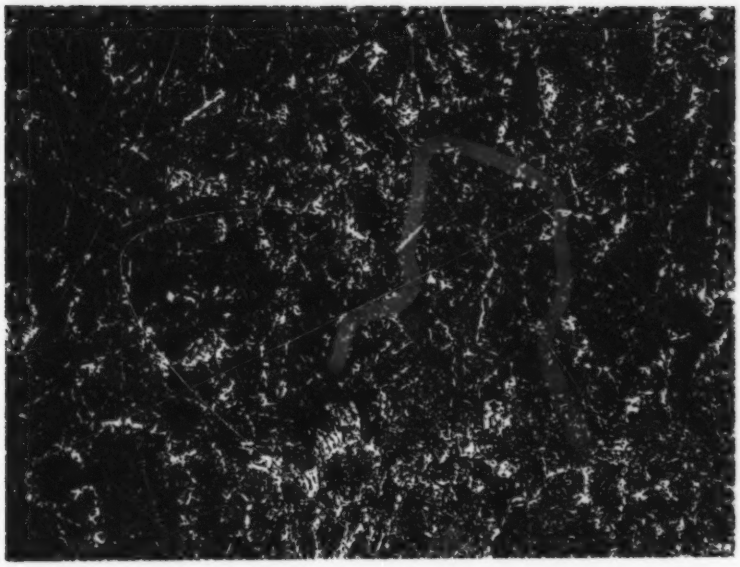

(a) (neg.17520)

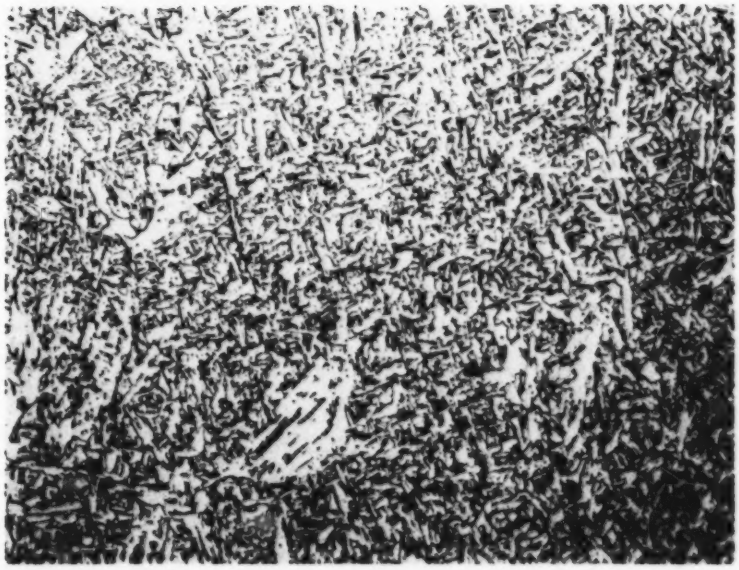

(b) (neg.17521)

Fig. 19 Microstructure of weld MA-1. Etch 2% Nital.

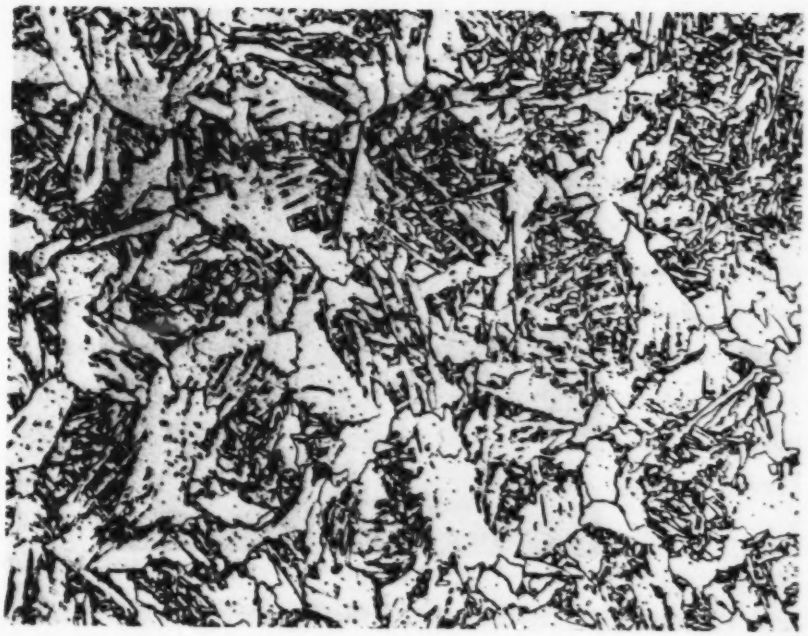

(a) coarse grain reheated (neg.17522)

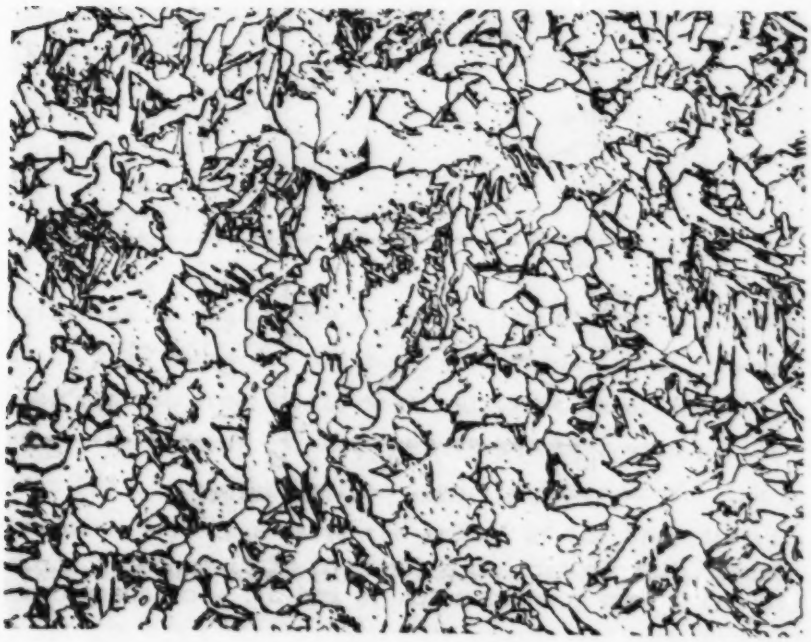

(b) fine grain reheated (neg.17523)

Fig. 20 Typical reheated weld metal microstructures. Etch 2% Nital.

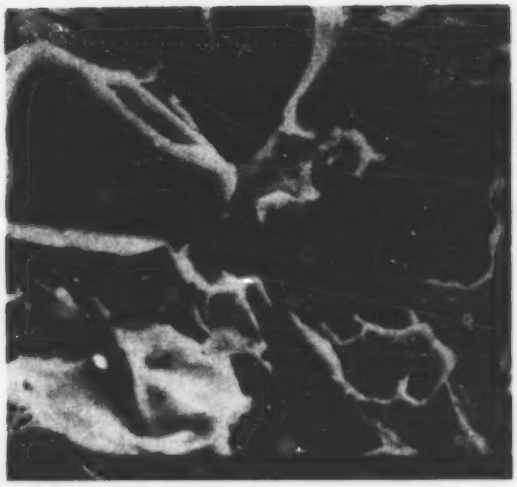

Fig. 21 Typical SEM fractograph showing initiation of cleavage failure from a large non-metallic inclusion. (neg.35 mm).

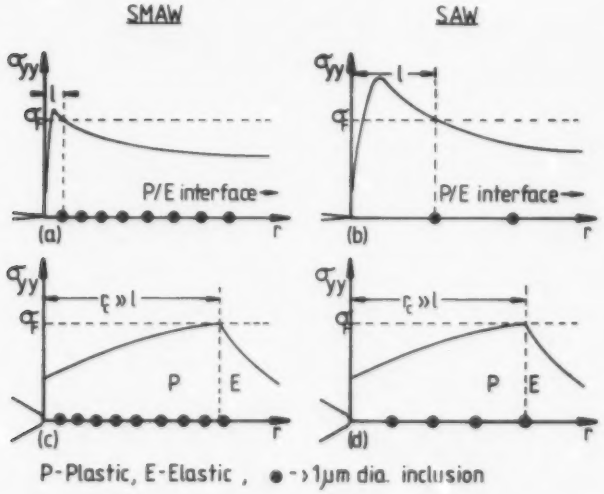

Fig. 22 Stress distribution as a function of distance, r, from sharp crack tip (a and b) and rounded notch (c and d). For sharp cracks, fracture occurs when the stress, σ_{yy}, exceeds the critical fracture stress, σ_F, over the distance " l ". For rounded notches, fracture occurs when the stress, σ_{yy}, reaches σ_F. (neg.14032)

APPENDIX A

Currently, for defect assessments, the procedure is to use the lowest value of three CTOD tests for a particular weld at the service temperature of interest. In the evaluations of the electrodes given in this report more than three tests were performed for each weld at both -30°C and -10°C. The reasoning for this was twofold. First, to obtain an indication of the effect of temperature on CTOD for each weld from the -10°C required for North Sea service to the -30°C required for East Coast Canada. Second, to obtain a slightly improved sample of the actual distribution of toughness for each weld (four or five test results provide more information about the true distribution compared to three). However, which value of CTOD, from the test results, are to be used for analysis and comparison? This value is dependent upon the level of risk that is acceptable that the weld may actually have a toughness lower than that measured.

The results for each temperature represent a known set of test results from an unknown distribution. To determine which value to use in an assessment a value above which $(1-\alpha)\%$ of the possible results lie is chosen, see Fig. A1. Results of tests which are below the $(1-\alpha)\%$ value, or threshold value (X), are regarded as failures. If the true distribution is just acceptable ($(1-\alpha)\%$ value = X) then the probability that all n test results lie above X is:

$$PR\ (n\ tests \geq X) = (1-\alpha)^n \qquad [1]$$

If the $(1-\alpha)\%$ value is just below X then [1] is the maximum probability that all n values will be above X. If the $(1-\alpha)\%$ value is well above X then [1] represents the minimum probability that all three results will be above X.

Currently, the minimum of three tests is interpreted as the value above which at least 50% of possible values lie. In other words, the minimum of three test results just lies above the median of the true distribution. Hence, the risk that the true value is less than the minimum of three tests is

$$PR\ (3\ tests \geq X) = (1-\alpha)^3 = (.5)^3 = .125$$

or 12.5%. As the sample size is increased (i.e. more tests are performed) the probability of all test results being greater than the median, X, increases. Conversely, the probability of obtaining a value below the median decreases. The threshold value, X, can be increased or decreased from the median value. For X greater than the median value the probability of the minimum of n tests being above X decreases while for X less than the median value, the probability of the minimum of n tests being above X increases. Examples of these are shown in Table A1. By using a value lower than the median for, say, a defect assessment, a level of conservatism is introduced. However, for the purposes of comparing different distributions or different batches (in this case different welds) the median value is desired. At this point one should note that for normal statistical assessments the highest risk of a hypothesis being wrong is often taken as 10% (90% confidence of being correct). The minimum of three test results is then interpreted as the value above which 46.4% of the possible results lie a value higher than the median. Hence, by taking the minimum of three tests as the median the confidence level is decreased to 87.5%.

For data sets larger than three test results several approaches may be used. The first is to interpret the lowest value of the test results as the value above which 50% of the possible results lie. In this case as the number of tests is increased, the risk of the true median being below the minimum of the test values decreases. Another approach is to use a value higher than the minimum of the test results while maintaining the same risk as that associated with using the minimum of three tests. Also, a combination of the above approaches may be used where a value higher than the minimum of the test results is used and the risk that the true median is below this value is improved (i.e.: equivalent to the lowest of, say, four rather than three tests).

In order to use the last two of the above approaches one needs to assess the probability of "r" or fewer values being less than the threshold value X. The probability of "r" values being less than X is given by the binomial distribution as

$$P(n-r \text{ tests } \geq X) = {}^{n}C_{r}\,\alpha^{r}(1-\alpha)^{n-r} \qquad [2]$$

where ${}^{n}C_{r}$ is given by

$$ {}^{n}C_{r} = \frac{n!}{r!(n-r)!} \qquad [3] $$

To obtain the probability of "r" or fewer values being less than X we sum the individual probabilities to give

$$ P(r \text{ or fewer EX}) = \sum_{i=0}^{r} {}^{n}C_{i}\ \alpha^{i}(1-\alpha)^{n-1} \qquad [4] $$

For the case of three samples the minimum value of the three was considered as being just above the median of the true distribution. Hence $(1-\alpha) = 0.5$ and the probability that the true median value was less than the minimum was calculated to be 0.125. Using the true median value for the threshold we can calculate, using [4], the probability of obtaining, say, one or fewer values below the median. The results of this calculation for sample sizes, n, ranging from three to 15 is shown in Table A2. From this table it is shown that for a set of six (n=6) test results, using the second lowest value, instead of the lowest, would be similar in risk, to using the lowest of three test values. (P(1 or fewer <X in 6 tests) = .1094 is just less than P (3 tests $\geq$X) = .125). However, for the cases of samples with four or five test values (n = 4 and n = 5) using the second lowest values would result in a higher risk than using the minimum of three tests. Hence, for the five tests at -30°C and four tests at -10°C for each weld the lowest value from each set will be used for comparison purposes. However, it is noted from Table A-1 that the risk of the true median value being below the minimum test values is reduced to 6.25% for n=4 and 3.12% for n=5.

Table A-1

P_r (n tests $\geq X$) = $(1-\alpha)^n$

	(1-α)					
n	.25	.50	.60	.70	.80	.90
3	.0156	.125	.2160	.3430	.5120	.7290
4	.0039	.0625	.1296	.2401	.4096	.6561
5	.0010	.0312	.0778	.1681	.3277	.5905
6	.0002	.0156	.0467	.1176	.2621	.5314
7	.000061	.0078	.0280	.0824	.2097	.4783
8	.000015	.0039	.0168	.0576	.1678	.4305
9	.0000038	.0020	.0101	.0404	.1342	.3874
10		.0010	.0060	.0282	.1074	.3487
11		.0005	.0036	.0198	.0859	.3138
12		.0002	.0022	.0138	.0687	.2824

Table A-2

P(1 or fewer <X) for X = true median value [$(1-\alpha) = 0.5$]

n	P(1 or fewer <X)
3	0.5
4	0.3125
5	0.1875
6	0.1094
7	0.0625
8	0.0352
9	0.0195
10	0.0107
11	0.0059
12	0.0032
13	0.0017
14	0.0009
15	0.0005